

**THE SYNTHESIS AND MODE OF
ACTION OF NPPB AND RELATED
COMPOUNDS**

A thesis submitted in partial fulfilment of the
requirements for the Degree

of Master of Science in Biochemistry

in the University of Canterbury

by Yukiyo Muto

University of Canterbury

2006

Table of Contents

Table of Contents	1
Acknowledgments	3
Abstract	4
List of Tables.....	6
List of Figures	7
Abbreviations and Definitions	8
Chapter 1 Introduction.....	10
1.1 Overview	10
1.2 Membrane Transport	11
1.3 Ion Channels in Plants	16
1.3.1 K ⁺ Channels	17
1.3.2 Cl ⁻ Channels.....	20
1.3.3 Ca ²⁺ Channels	20
1.4 Ion Channel Inhibitors	24
1.4.1 NPPB and Niflumic acid	24
1.4.2 NPPB and Related Compounds	26
1.5 The Techniques of Protein Channel Study	29
1.5.1 Chemical Synthesis	29
1.5.2 Cytoplasmic Streaming	37
1.5.3 Turgor Regulation.....	38
1.5.4 Aequorin Technology.....	39
Chapter 2 Material and Methods.....	44
2.1 Sample Collection.....	44
2.2 Chemical Synthesis.....	44
2.2.1 NPPB.....	44
2.2.2 PPAB.....	47
2.2.3 HANB	48
2.2.4 HANB-2.....	49
2.3 Cytoplasmic Streaming.....	50
2.3.1 Sample Preparation.....	50
2.3.2 Streaming Rate Measurement	51
2.4 Turgor Regulation.....	52
2.4.1 Sample Preparation.....	52
2.4.2 Pressure Probe Measurements.....	53
2.4.3 Test Solutions	56
2.4.4 Osmotic Potential	57
2.5 Cytosolic Free Calcium Analysis	58
2.5.1 Aequorin Transformed Cells.....	58

2.5.2 Luminescence Measurements	59
Chapter 3 Results	61
3.1 Chemical Synthesis.....	61
3.1.1 NPPB.....	61
3.1.2 PPAB.....	64
3.1.3 HANB	64
3.1.4 HANB-2.....	66
3.2 Cytoplasmic Streaming.....	68
3.3 Turgor Regulation.....	76
3.4 Cytosolic Free Calcium Analysis	83
3.4.1 NPPB.....	85
3.4.2 PPAB.....	87
3.4.3 HANB	87
Chapter 4 Discussion	91
4.1 Chemical Synthesis.....	91
4.1.1 NPPB.....	91
4.1.2 PPAB.....	92
4.1.3 HANB	92
4.1.4 HANB-2.....	92
4.2 Cytoplasmic Streaming.....	93
4.3 Turgor Regulation.....	95
4.3.1 Turgor Pressure in Resting State.....	95
4.3.2 Hypertonic Regulation.....	96
4.3.3 Effects of Ion channel inhibitors	98
4.4 Cytosolic Free Calcium Analysis	100
Chapter 5 Conclusions and Future Research.....	103
References	105

Acknowledgments

I would like to thank my supervisor, Ashley Garrill and my associate supervisor, Andrew Abell, for their academic and technical support throughout my research. Also thanks to Stephen McNabb for great support during chemical synthesis experiments.

Thanks to the members of both the School of Biological Sciences and the Department of Chemistry for contributing to a great working environment. Also thanks to Craig Galilee for technical assistance, and thanks to Colin McLay for helping me regarding administration of this MSc thesis.

Also thanks to Francois Bouteau for associating with this research and thanks to Mark R Knight and Alain Pugin for providing the transformed cell lines.

Big thanks to my partner, Andrew Gorman for his great support.

Abstract

5-nitro-2-(3-phenylpropylamino)-benzoic acid (NPPB) was normally recognised as a Cl⁻ channel inhibitor, but its specificity is in question, since an inhibitory effect against K⁺ channels has been reported. To identify the significance of the molecules structural components, NPPB and related compounds, such as 2-(3-phenylpropylamino) benzoic acid (PPAB), 5-nitro-2-heptylamino benzoic acid (HANB) and 2-nitro-5-heptylamino benzoic acid (HANB-2) were synthesised by reductive amination using various aldehydes and amines.

Using internodal cells of the giant green Characean algae, *Nitella hookeri*, the effects of NPPB and related compounds on cytoplasmic streaming and turgor regulation were determined. Previous experiments stated that cytoplasmic streaming was sensitive to NPPB, PPAB and HANB with IC₅₀ values of 24µmol/L, 455µmol/L, and 6.4mmol/L, respectively. In this report, the IC₅₀ values of purchased NPPB and niflumic acid were found to be 88.65µmol/L and 121.82µmol/L, respectively. Although the IC₅₀ value of purchased NPPB showed a slight difference from that of synthesised NPPB, the results of the cytoplasmic streaming experiment indicated the possibility of this analysis to be a simple assay system for analysing the effects of structural modification to ion channel inhibitors on their biological activity. Moreover, NPPB and PPAB seem to stimulate regulation of turgor pressure under hyperosmotic shock, which can be explained by a blockage of K⁺ efflux during osmotic stress leading to faster recovery of turgor regulation. Additionally, the results of cytosolic free Ca²⁺ analysis using aequorin technology also suggested that the possibility of this analysis to be used as a more direct measure of the inhibitory effect, while the cytoplasmic streaming analysis is a more indirect method.

The preliminary results from this research suggest the significance of the simple assay systems for analysing the effects of structural modification ion channel inhibitors, which can be used for future study regarding ion channel structures.

List of Tables

1.1 Calcium-permeable channels in the plasma membrane of plant cells.

3.1 NMR data of NPPB

3.2 NMR data of PPAB

3.3 NMR data of HANB

3.4 NMR and IR data of HANB-2

3.5 The effect of NPPB (pH 8) on cytoplasmic streaming rate.

3.6 The effect of NPPB (pH 10) on cytoplasmic streaming rate.

3.7 The effect of Niflumic acid (pH 8) on cytoplasmic streaming rate.

3.8 The effect of NPPB on turgor regulation in hyperosmotic solution.

3.9 The effect of PPAB on turgor regulation in hyperosmotic solution.

List of Figures

- 1.1** Summary of membrane transport.
- 1.2** Action potentials in higher plants.
- 1.3** Structure significance of NPPB.
- 1.4** Generalized scheme of reductive amination.
- 1.5** Generalised scheme of reductive amination to form secondary amine.
- 1.6** NPPB synthesis
- 1.7** PPAB synthesis.
- 1.8** HANB synthesis
- 1.9** HANB-2 synthesis
- 1.10** Mechanism of light emission by aequorin upon Ca^{2+} binding.
- 1.11** Targeting aequorin into plant cells.
- 2.1** Pressure probe for turgor pressure measurement.
- 3.1** Dose-response curve for NPPB in pH 8 APW.
- 3.2** Dose-response curve for NPPB in pH 10 APW.
- 3.3** Dose-response curve for Niflumic acid in pH 8 APW.
- 3.4** The effect of NPPB on turgor regulation in the hyperosmotic solution.
- 3.5** The effect of PPAB on turgor regulation in the hyperosmotic solution.
- 3.6** The average increase of the concentration of cytosolic free Ca^{2+} in aequorin transformed cells with/without a calcium surrogate (La^{3+}).
- 3.7** The effects of NPPB on the concentration of cytosolic free Ca^{2+} in aequorin transformed cells.
- 3.8** The effects of PPAB on the concentration of cytosolic free Ca^{2+} in aequorin transformed cells.
- 3.9** The effects of HANB on the concentration of cytosolic free Ca^{2+} in aequorin transformed cells.
- 4.1** A model illustrating pathways of fast turgor adjustment in Arabidopsis root cells.

Abbreviations and Definitions

APW	Artificial pond water
Arom	Aromatic structure
ATP	Adenosine triphosphate
Ca²⁺	Calcium ion
CFTR	Cystic Fibrosis Transmembrane conductance Regulator
Cl⁻	Chloride ion
dd	doublet-doublet
HANB	5-nitro-2-heptylamino benzoic acid.
HANB-2	2-nitro-5-heptylamino benzoic acid
HCl	Hydrochloric acid
Hz	Hertz
IC₅₀	Concentration of inhibitor to halve maximum effect
IR	Infrared spectra
J	Coupling constant
K⁺	Potassium ion
LEAC	Large-conductance Elicitor-Activated Channel
M	Molar (moles per litre)
m	multiplet
MgSO₄	Magnesium Sulphate
mM	Millimolar
MS	Mass Spectra
Na⁺	Sodium ion

NaBH₃CN	Sodium Cyanoborohydride
Niflumic acid	Trifluoromethyl-3-phenylamino-2-nicotinic acid
NMR	Nuclear Magnetic Resonance
NPPB	5-nitro-2-(3-phenylpropylamino) benzoic acid
pH	Potential of Hydrogen
PPAB	2-(3-phenylpropylamino) benzoic acid
s	singlet
SD	Standard Deviation
TEA	Tetraethylammonium
t	triplet
Ti(OiPr)₄	Titanium(IV)isopropoxide
TLC	Thin Layer Chromatography
TTX	Tetrodoxin
UV	Ultra Violet
ZnCl₂	Zinc chloride

Chapter 1 Introduction

1.1 Overview

The alga used in this thesis was *Nitella hookeri*. *Nitella* is one of the giant green Characean algae belonging to the kingdom Protista. It has axial internodes that are up to 3mm in diameter and up to 15cm long. Because of these large internodal cells, the Characean algae are very useful organism to work with physiological experiments, such as observing cytoplasmic streaming, turgor regulation, patch clamping and the more classical voltage clamping. Cytoplasmic streaming has been extensively studied with the large cells of Characean algae, where rates of up to 75 μ m per second have been measured (1). The large internodal cells are easy to impale with the micropipettes used in single cell pressure probe work, thus allowing measurement of turgor regulation. Furthermore the advantage of using Characean algae in patch clamping is that the large cytoplasmic droplets, which readily form tight resistance seals, can be easily obtained without any enzymatic disruption (2).

Ion channels are proteins, which facilitate the passive movement of ions, such as Na⁺, K⁺, Cl⁻, Ca²⁺, across a cell membrane. Such movements play significant roles in a number of cellular processes that are essential for life. The malfunction of ion channels underlies many diseases, such as atherosclerosis and cystic fibrosis. Studies of the biochemistry and physiological function of ion channels are thus crucial for understanding their various biological functions and the mechanistic of such diseases.

Many naturally occurring toxins and venoms target ion channels and have been used in such studies. Synthetic channel blockers are also useful for such work. 5-nitro-2-(3-phenylpropylamino)-benzoic acid (NPPB) an arylaminobenzoate, and related compounds have been widely used to study Cl⁻ channels in both plant and animal cells. However they have recently been found in certain plant cell types to be more potent blockers of K⁺ channels.

In this research, the significance of NPPB as an ion channel inhibitor was determined by observing the inhibitory effects of NPPB and related compounds on cytoplasmic streaming, turgor regulation, and cytosolic free calcium ion concentration. Such studies are possible through a unique synthetic technique involving the synthesis of NPPB and related compounds by reductive amination using various aldehydes and amines. The observation of the degree of inhibition among the analogues would identify the structural components required for inhibition which gives further information regarding channel structure for any future study.

1.2 Membrane Transport

All cells are enclosed by a membrane, which provides a boundary to separate the cytoplasm from the cell wall and the external environment (1). This plasma membrane is composed of phospholipids and proteins. The phospholipids are a class of lipids which have two fatty acids and phosphates which are covalently attached to a glycerol. This molecular structure provides non-polar region at the glycerol head and polar region at the fatty acid's tail. In an aqueous environment, the phospholipids spontaneously form a bilayer structure, which consists of a back-to-back arrangement of two monolayers (3). The phospholipid bilayer has a hydrophilic surface and a hydrophobic

core. This hydrophobic property of the plasma membrane and the close association of the individual phospholipids serve as a barrier to the passage of molecules that are large, have polarity or carry charge (4). This barrier is crucial for the survival of any cell, and enables the maintenance of differential concentration of various solutes between the cell interior and the extracellular fluid.

The creation of such differential concentrations requires the movement of molecules and ions between inside and outside of cells through the plasma membrane, a process that is known as membrane transport. Membrane transport processes are vitally important for all life forms. Obviously, cells have to import nutrient molecules to nourish themselves and to move waste products and toxic substances out. Moreover, various ions must be transported through the plasma membrane to maintain concentration gradients and to enable cell signaling processes. The importance of such gradients is reflected in the amount of energy that cells devote to their generation and maintenance, for example yeast cells devote around 50% of their ATP to the operation of the H^+ -ATPase that is responsible for the a large H^+ gradient across the plasma membrane. Similarly in the animal brain around one third of ATP is used to fuel the Na^+/K^+ ATPase; the Na^+ and K^+ gradients across the plasma membrane thus created mediate the transmission of nerve impulses and the normal functions of the brain and other organs, such as heart, kidneys, and liver. Other crucial movements of ions include Cl^- transport which is involved in fluid secretion in the intestine and airways (5) and the storage and release of Ca^{2+} from cells which is used to control muscle contraction, and also the response of many cells to hormonal or enzymatic signals.

Various proteins embedded in the plasma membrane are responsible for the selective transport of solutes across the membrane summarized in Fig 1.1. These are known as transport proteins and there are two major types, which are carriers and channels. In carrier mediated transport, the carrier proteins bind the transported molecule, which is followed by conformational change in the protein. This conformational change brings the transported to the other side of the membrane. The transport will be completed by the dissociation of the substance, either into the cell or away from the cell depending on the direction of the transport process. There are two types of carrier mediated transport. When the transported molecule moves down its electrochemical gradient, the process is called passive transport or facilitated diffusion. The second type of carrier mediated transport is the movement of a molecule up or against its electrochemical or concentration gradient. This is called active transport and requires a driving force, such as hydrolysis of ATP or the diffusion of other molecules. A membrane transport protein, which requires energy from the hydrolysis of ATP, is generally called a pump. A membrane transport protein, which uses the energy derived from the diffusion of other molecules such as H^+ or Na^+ , is known as co-transporter or exchanger.

Membrane channel proteins include gap junctions, porins, and ion channels. Gap junctions form pores between two adjacent cells and enable molecules to move between these cells by simple diffusion. The porins are transport protein found in the outer membranes of Gram negative bacteria and mitochondria. Both are generally, non-specific transport protein.

The ion channels are transmembrane proteins that facilitate ion diffusion across a membrane by forming an aqueous macromolecular pore. When the pore is open, it allows ions to pass through the water filled hydrophilic pore.

The size of a pore and the density of surface charges of its interior lining determine its transport specificity. The amino acid residues in the interior

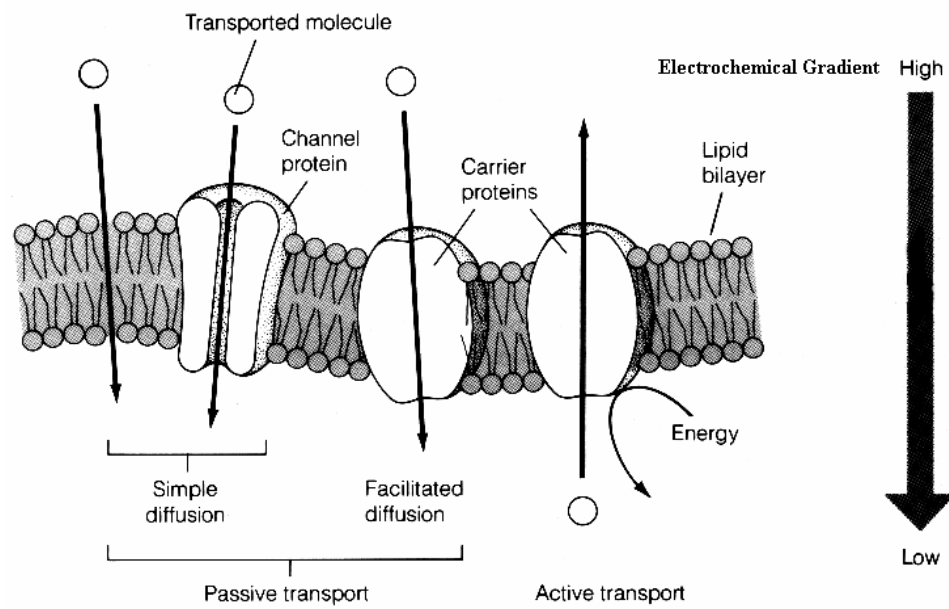


Figure 1.1 Summary of membrane transport. (Adapted from (6))

lining of the pore interact with ions to form thermodynamic energy barriers to make the pore to be selective to the certain ions. However, no channel is perfectly selective. The Na^+ channel of animal axons is able to pass NH_4^+ and is even slightly permeable to K^+ as well (7).

The opening and closing of the pore of an ion channel is controlled by a gating mechanism performed by a conformational change of the channel protein. The conformational change can be activated by several factors, which distinguish the type of channels (8).

Voltage-dependent channels are activated by an increase or a decrease in the membrane potential. Such changes are detected and responded to by certain charged amino acid residues in the protein that act as a voltage sensor. These residues shift position within the channel protein in response to membrane potential changes (7). These are almost ubiquitous and found in both animal and plant cells.

Ligand-gated channels are subject to conformational change upon the binding of an extracellular factor, such as a hormone or a neurotransmitter. This process is very similar to an enzyme-receptor interaction.

Mechanosensitive channels are activated by the mechanical stimuli, such as tension for plant cells. In plant cells, tension from the cell wall is transmitted to the channel via possible integrin linkers and cytoskeletal elements, such as F-actin. Such transmission may affect a conformational change of the mechanosensitive channels.

1.3 Ion Channels in Plants

Although plants lack the nervous system and organs of higher animals which have served as model systems in classical studies of membrane bioenergetics (7), ion channels in plant nonetheless play crucial roles in growth, osmoregulation, nutrition and behavioural responses to the environment. There are several types of ion channels that are known or are believed to occur in plant cells. Some of them are known to be involved in action potentials, but many of them have other functions which are not known yet. In plant cells, the ion channels, which are involved with action potential, mediate sensory-motor responses, such as opening and closing stomata in response to humidity changes, moving leaves to follow sunlight, moving floral parts in pollination, and turning the shoots toward a vertical direction.

Electrical excitability and action potentials are well documented in some algae and higher plants (9) and they are often initiated by mechanical stimulation of sensory hairs or floral parts. Some plants also show quick response, which is easy to observe by eyes, to the mechanical stimulation such as the rapid trap closure of Venus's-flytrap and the folding leaves and petioles in the sensitive plants including *Mimosa pudica*. The observed action potentials in those plants are shown in Fig 1.2. In *Mimosa pudica*, this response is due to the function of a Cl^- channel. The increase in the membrane potential is achieved by a Cl^- efflux into the extracellular medium, with the drop to the resting potential achieved by a Cl^- influx (10). This depolarizing rise from a negative resting potential can spread through hundreds of adjacent cells over distances of as much as several meters. On the other hand, the action potential of Venus's-flytrap seems to be involved with Ca^{2+} conductance. The

rising phase of membrane potential is due to the Ca^{2+} influx, and the efflux leads to the resting phase.

Probably the most studied plant action potential is that of the Characian algae, specifically the giant internodal cells of *Chara* and *Nitella*. The cytoplasmic streaming of the internodal cells is arrested by regenerative action potentials, which is regulated by mainly Cl^- and K^+ movement. Excitation begins with the activation of a voltage-gated Ca^{2+} channel. Ca^{2+} entry activates Cl^- channel. The efflux of Cl^- ions is responsible for the depolarizing phase, and the efflux of K^+ ions is responsible for the repolarizing phase (11).

The resting membrane potential of plants and fungi is maintained by currents driven by ion pumps and the proton ATPase, rather than ion channels. The strong negative membrane potential is normally due to the expulsion of K^+ . Many plants and fungi cells are surrounded by dilute solutions, therefore the active transport of ions by the pumps create large concentration gradients. However the ion channels which are activated by mechanical stimulation can thus allow large ion fluxes and these can change the salt content in the cell allowing the cell to shrink or swell depending on the environmental conditions.

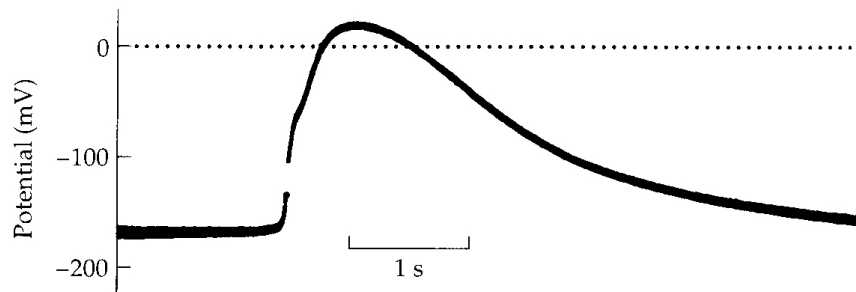
In plant cells, such fluxes, along with changes in the concentration of compatible solutes such as sugar alcohols, can lead to turgor regulation.

1.3.1 K^+ Channels

There are several ion channels that have been identified in *Nitella* sp, and most of these are involved in the generation of action potentials (12,13). The

action potential across the plasmalemma of *Nitella* sp provides the ability to control turgor and cellular ionic composition, which is necessary for survive in

(A) SENSITIVE PLANT



(B) VENUS'S-FLYTRAP

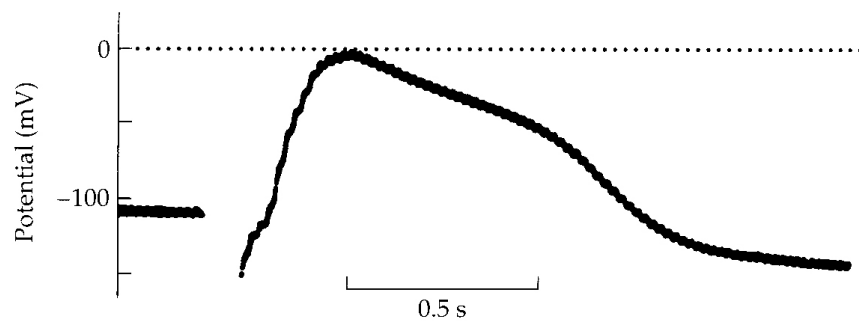


Figure 1.2 Action potentials in higher plants.

Action potentials recorded intracellularly from (A) the sensitive plant *Mimosa pudica*, and (B) the Venus's-flytrap *Dionaea muscipula*. (Adapted from (7))

fresh water. Potassium channels that are involved in the repolarization phase of the action potential are known as Ca^{2+} activated Maxi- K^+ channels. The name of Maxi- K^+ refers to the large conductance.

The Ca^{2+} activated Maxi- K^+ channel is also characteristic of the plasmalemma of *Chara* where it dominates channel events in resting cells, when the cell is in the so-called K-state. This is the state when cells are depolarized and the potential difference across the membrane stays near the K^+ equilibrium potential (14).

The Maxi- K^+ channels of the tonoplast show different characteristics from those of in the plasmalemma. They behave like animal Maxi- K^+ channels, although these are inwardly rectifying. Normally K^+ channels in the tonoplast have a higher conductance and lower specificity than the K^+ channels in the plasmalemma. However, according to patch clamp studies under various ionic conditions, the Maxi- K^+ channels of the tonoplast can show high specificity and are virtually impermeable to Na^+ and Cl^- ions (15). Moreover, the Maxi- K^+ channels of the tonoplast are blocked by high concentrations of cytosolic Ca^{2+} , while those of the plasmalemma are activated by Ca^{2+} (16). The channels of the tonoplast are activated by voltage and micro molar cytosolic Ca^{2+} (17,18). They are also sensitive to pH. Lowering the pH of the bathing solution, which virtually mimics the vacuolar environment, from an almost neutral level to values below pH 7, induces a significant but reversible decrease in channel activity, whereas channel conductance remains largely unaffected (19). This pH sensitivity predicts that the structural features of Characean maxi- K^+ channels, includes a voltage sensor and negatively charged residues in neighboring transmembrane domains whose stabilizing function may be altered by protonation.

1.3.2 Cl⁻ Channels

Chloride channels in plasma membrane of plant cells are often responsible for an amplification of the action potential. The Cl⁻ channels are probably activated by a rise in cytoplasmic Ca²⁺ levels (20). Some Cl⁻ channels have been identified in the *Characean* tonoplast, and most of them are also sensitive to an increase in cytoplasmic Ca²⁺ level (21).

In the plasma membrane of *Chara*, Cl⁻ channels which open upon hyperpolarisation and at low external pH have been found (22,23). At low external pH, these Cl⁻ channels allow the efflux of Cl⁻ ions. This efflux lowers the potential difference across the membrane and keeps the proton-motive force constant by controlling the activity of the H⁺ pump. Also the channels, which are selective for Cl⁻ over K⁺, open upon hyperpolarisation and have been identified in the plasma membrane of *Chara* by steady-state single-channel recordings using the patch clamp technique (2).

Although more work about the specificity of the channels is eagerly awaited, there has been some preliminary evidence for the presence of stretch activated Cl⁻ channels in the plant plasma membrane (24).

1.3.3 Ca²⁺ Channels

Calcium is not only an essential plant nutrient that is needed to maintain structure, but also it is firmly recognized as a second messenger in numerous plant signaling pathways. Although calcium is an essential plant nutrient, high concentrations of cytosolic free Ca²⁺ can be cytotoxic and have been implicated in apoptosis. Under resting conditions, the concentration of cytosolic Ca²⁺ is maintained between 100 and 200 nM (25), which is 10⁴ times less than in the apoplastic fluid and 10⁴ to 10⁵ times less than in cellular organelles. This submicromolar concentration of cytosolic Ca²⁺ is maintained

by Ca^{2+} -ATPases and $\text{H}^+/\text{Ca}^{2+}$ -antiporters (26). Therefore any sudden increase in cytosolic free Ca^{2+} , provided from extracellular medium or vacuole and other organelles, is thought to be a key component of several plant signaling pathways. This special and temporal change in the concentration of cytosolic free Ca^{2+} is referred to as calcium signature, and it is caused by several stimulus such as pathogens, oxidative stress, light, osmotic stress, and mechanical stimulations.

Ca^{2+} can be transported rapidly through Ca^{2+} permeable ion channels. Calcium channels have been characterized in the plasma membrane, endoplasmic reticulum, tonoplast, nuclear and plasmid membranes of plant cells (27). The Ca^{2+} channels in the plasma membrane are divided into several types: depolarization-activated; hyperpolarisation-activated; and voltage-insensitive channels. Then, these may be subdivided on the basis of their permeability of other ions, and sensitivity to inhibitors (Table1.1).

The depolarization-activated Ca^{2+} channels are found in the plasma membrane of all plant root cells, leaf mesophyll cells and suspension-cultured cells. The characteristic of Ca^{2+} currents through this type of channels was first identified described in protoplasts from suspension-cultured cells from carrot (28), followed by the protoplasts from leaf mesophyll and root cells of *Arabidopsis* (29). The Ca^{2+} current is activated by depolarization of the membrane potential to the positive voltages that are more positive than around over -140mV. Then once activated it exhibits slow and reversible inactivation at extreme negative voltages. So the ion flux through the depolarization-activated Ca^{2+} channels is likely to be a consequence of voltage dependent conformational changes in the channel protein structure, rather than for example phosphorylation and dephosphorylation. There are two

Name	Tissue	Permeability	Inhibitors of Ca ²⁺ flux
Depolarisation-activated			
DACC	Carrot cell suspension	Ca, Ba, Sr, Mg	
DACC	<i>Arabidopsis</i> root	Ca	Mibefradil
	<i>Vicia faba</i> guard cell	Ca, K	
<i>rca</i>	Wheat root	Na, Cs, K, Li, Rb	Ruthenium red, verapamil, diltiazem, Ni ²⁺ , Al ³⁺ , La ³⁺ , Gd ³⁺ , TEA ⁺
		Ba, Sr, Ca, Co, Mg, Zn, Mn, Ni, Cd, Cu	
VDCC2	Rye root	Cs, K, Rb, Na	Verapamil, La ³⁺ , TEA ⁺
		Ba, Ca	
Maxi-cation	Rye root	K, Rb, Cs, Na, Li	Ruthenium red
		Ba, Sr, Ca, Mg, Co, Mn	
Hyperpolarisation-activated			
Mechano-sensitive	<i>Vicia faba</i> guard cell	Ca	
Mechano-sensitive	Onion bulb epidermis	Ca, K	Al, Gd ³⁺ , La ³⁺
	<i>Vicia faba</i> guard cell	Ca	Gd ³⁺ , calcicluidine
	<i>Arabidopsis</i> root	Ca	Al ³⁺
	<i>Arabidopsis</i> leaf mesophy	Ba, Ca	[Ca ²⁺] _{cyt}
Elicitor-activated	Tomato cell suspension	Ba, Ca	La ³⁺ , nifedipine
Voltage-independent			
LEAC	Parsley cell suspension	Ca, K	La ³⁺ , Gd ³⁺

Table 1.1 Calcium-permeable channels in the plasma membrane of plant cells. (Adapted from (27))

depolarization-activated Ca^{2+} channels that have been identified, which these are the *rca* or VDCC2 channel and the maxi cation channel. Both are permeable not only Ca^{2+} , but also a wide variety of monovalent and divalent cations, unlike L-type Ca^{2+} channels in animal cells. Under physiological ionic conditions, Ca^{2+} influx is likely to dominate the ionic fluxes through *rca*/VDCC2 and maxi cation channels, which necessitates their primary classification as Ca^{2+} channel.

The hyperpolarisation-activated Ca^{2+} channels were identified in protoplasts from various cell types, which are involved with various physiological functions, such as stomatal closure and hyphal tip growth. They are mainly mechanosensitive ion channels, which are activated by mechanical stresses induced by gravity, touch or flexure. It has been reported that the mechanosensitive Ca^{2+} channels are involved with cell expansion and morphogenesis, such as the elongation of root hairs (30) and pollen tubes (31). There is one elicitor activated channel that has been documented as a hyperpolarisation-activated Ca^{2+} channels. The Ca^{2+} channel, activated at voltages more negative than -120mV, was characterized in protoplasts from tomato (*Lycopersicon esculentum L*) suspension cultured cells. The Ca^{2+} influx through the elicitor activated channel appears to be an early event in the initiation of defense responses to pathogens.

The voltage-insensitive channels are recognized as elicitor activated channels. A large-conductance elicitor-activated channel (LEAC) has been characterized in protoplasts from parsley (*Petroselinum crispum*) suspension-cultured cells (32). A Ca^{2+} influx was observed in the presence of an oligopeptide elicitor, derived from a cell wall protein of the phytopathogenic fungus *Phytophthora sojae*. This elicitor activated the channel to allow the

Ca²⁺ influx, but this activation was not dependant on the membrane potential. The structural features of the elicitor, which activates LEAC, are also crucial for both receptor binding and induction of defense related gene expression. Therefore, Zimmermann et al have suggested that the activation of LEAC is causally related to the plant defense pathways.

1.4 Ion Channel Inhibitors

The malfunction of ion channels underlies many diseases, such as cardiac arrhythmias, atherosclerosis and cystic fibrosis. Studies of the biochemistry and physiological function of ion channels are thus crucial for understanding their various biological functions and the mechanistics of such diseases. Many naturally occurring toxins and venoms that target ion channels have been used in such studies. Synthetic channel blockers are also useful for such work. The classic example of this is the use of tetraethylammonium (TEA) and tetrodotoxin (TTX). TEA inhibits K⁺ channels while TTX inhibits Na⁺ channels in the plasma membrane of animal cells (7). Due to their high specificity, these inhibitors were used for identifying the involvement of K⁺ and Na⁺ channels in the action potential of nerve cells. Thus, ion channel inhibitors are important tools for characterising the behavior and physiological function of ion channels.

1.4.1 NPPB and Niflumic acid

This report focuses on NPPB (5-nitro-2-(3-phenylpropylamino)-benzoic acid) and related compounds. For cytoplasmic streaming experiments, niflumic acid (trifluoromethyl-3-phenylamino-2-nicotinic acid) was also used. Originally, NPPB was developed as an anti-viral agent, while niflumic acid

was synthesized as an anti-inflammatory compounds (33,34). Both of these compounds are commercially available.

The first use of NPPB and niflumic acid on plants was on guard cells of the broad bean *Vicia fabia* as a voltage-dependent anion channel blocker (35). Since then, NPPB and niflumic acid have been used as specific inhibitors of anion channels, in particular Cl⁻ channels. The specific blockage of anion channels can give an experimental situation where only cation channels open. Thus, NPPB and niflumic acid have actually been used to study cation channel function. Examples include the inward rectifying cation current in the green alga *Eremosphaera viridus* (studied using NPPB (36)) and the action potential of *Chara* (studied with niflumic acid (37)). In animal cells the use of NPPB and niflumic acid as specific Cl⁻ channel inhibitors has led to a hypothesis that the activity of Cl⁻ channels participate in the regulation of Ca²⁺ induced erythrocyte apoptosis (38).

Despite the usage described above, the specificity of NPPB and niflumic acid has been questioned. It has been reported that NPPB is not only a highly potent blocker of epithelial Cl⁻ channels, but also a blocker of the intermediate-conductance Ca²⁺-activated K⁺ current in human leukemic HL-60 and glioblastoma GL-15 cell lines (39). With respect to niflumic acid, it also has been reported that large conductance calcium-activated K⁺ channels were rapidly activated by niflumic acid in a dose-dependent and reversible manner (40). It has also reported that niflumic acid blocks Ca²⁺-activated non-selective cation channels in pancreatic cells (41). Moreover, NPPB and niflumic acid may also involve with Ca²⁺ signaling. Increase of intracellular Ca²⁺ concentration in rat pulmonary artery smooth muscle cells by NPPB and niflumic acid has been reported (42). More pertinent to the current study, is the

specificity of NPPB and niflumic acid in plant cells and this question has also been raised. In the plasma membrane of root protoplasts from the wheat *Triticum aestivum*, NPPB and niflumic acid showed higher potency towards K^+ channels than to Cl^- channels(43).

1.4.2 NPPB and Related Compounds

The structural feature of NPPB is summarized in Fig 1.3. The important components of the molecule for acting as a Cl^- channel blocker are thought to be the anionic group, the electron withdrawing group, the amino bridge, and an apolar interaction site. The carboxylate of NPPB acts as an anionic group which is ionized at physiological pH. Other anionic groups such as sulfonyl urea are able to replace the carboxylate group, but they are less effective or have very little effect, as in the case of sulfonates. An *m*-nitro substitution on the benzoate moiety provides an electron withdrawing group which increases the potency as Cl^- channel blocker. The amino bridge is necessary for NPPB function, and it can not be replaced by either oxygen, phosphorus, or carbon. The apolar interaction site is also required and structural modifications to this site are providing interesting information for the study of ion channels with NPPB. As well as the structural components of molecule, the spacer between the structures also appears to be important. It has been reported that the distances between the carboxylate group and the amino group, between the nitro group and the carboxylate group, and between the phenyl ring and the amino group are very critical (44).

The relevance of the structural features of NPPB to activity has been well documented using the cystic fibrosis transmembrane conductance regulator protein (CFTR) and findings support the suggestions of Greger *et al* as summarized in the preceding paragraph. CFTR is a cAMP-activated

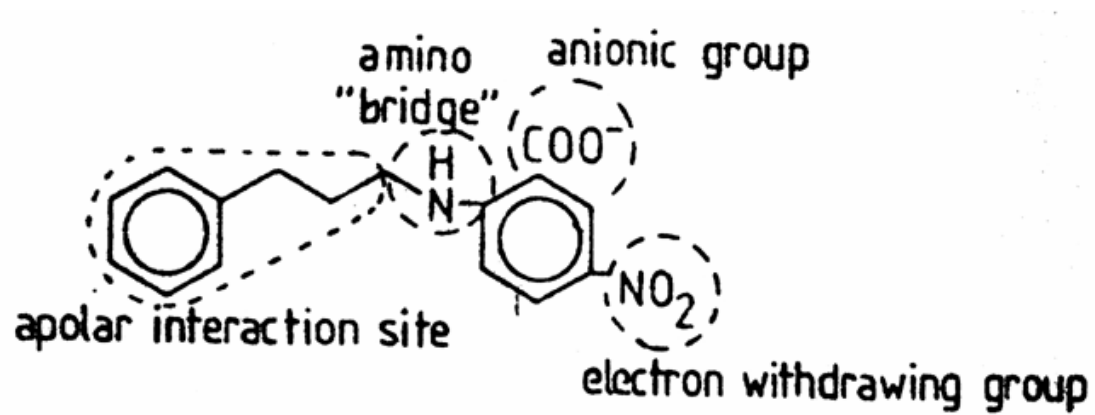


Figure 1.3 Structure significance of NPPB. (Adapted from (44))

Cl⁻ channel expressed in epithelial cells in mammalian airways, intestine, pancreas, sweat glands and testis. It plays a role in the regulation of fluid secretion.

Cystic fibrosis is a hereditary lethal disease caused by mutations in the gene encoding CFTR protein. Because of the limited information of CFTR structure and the inadequacy of available inhibitors as lead compounds, the screening technique with diverse chemical compounds has been used to identify and characterize inhibitors of CFTR Cl⁻ channel function (5). NPPB has been shown to inhibit the cardiac isoforms of CFTR in a voltage and pH dependent manner (45).

The structural components of NPPB which are crucial for blockage of the CFTR Cl⁻ channel have been identified by modification of the structure of NPPB (46). The removal of the electron withdrawing group on the benzoate ring form PPAB (2-(3-phenylpropylamino) benzoic acid) has been shown to drastically decrease drug potency. The absence of the benzoate ring (2-amino-4-phenylbutyric acid) resulted in a complete absence of inhibitory function. Both of these structural modifications interfere with the acidity of the molecule by destabilizing the carboxylate anion state. Since strong pH dependence for inhibition was observed, the acidity of the benzoate ring is thought to be one of the important factors that contribute to drug potency.

On the other hand, the absence of the phenyl ring, giving the compound 5-nitro-2-butylamino benzoic acid, showed only a relatively small change in inhibition. Moreover, the additional phenyl ring resulted in enhanced drug potency. Since this structural component acts via an apolar interaction, the presence of hydrophobic phenyl ring promotes drug interactions with the lipid

membrane. Using the same reasoning, increasing the alkyl chain length also enhances hydrophobic interactions and may increase the drug potency. Such modification has been reported to increase inhibition of Shaker K⁺ channels (47).

Thus observations of the degree of inhibition among these ion channel inhibitors and structural related analogues can identify the structural components required for inhibition which can give information regarding channel structure.

In this report three NPPB related compounds, PPAB, 5-nitro-2-heptylamino benzoic acid (HANB) and 2-nitro-5-heptylamino benzoic acid (HANB-2) were of interest. Because these compounds are not commercially available, the synthesis of these compounds is also discussed.

1.5 The Techniques of Protein Channel Study

1.5.1 Chemical Synthesis

5-nitro-2-(3-phenylpropylamino) benzoic acid (NPPB) is the ion channel inhibitor that is the focus of this research. The previously published synthesis of NPPB involves an aliphatic substitution reaction using 2-chloro-5-nitrobenzoic acid and 3-phenylpropylamine as a nucleophilic reagent. The electron withdrawing properties of the carboxylate and nitro substituents activate the usually unreactive benzene ring, and then this reaction leads to the substitution of the chlorine group to form NPPB. However, this reaction requires elevated temperature up to 145°C (48) and is sensitive to substituent effect for the proper positioning of nitro group to form NPPB (49).

By contrast, the method presented in this research is based on a simple

reductive amination of an aldehyde with a primary amine, which is a relatively simple procedure and does not require a high temperature (50). The reductive amination process, which converts aldehydes and ketones to amines, proceeds through the formation of an imine. The aldehydes and ketones are converted to the primary amines through catalytic or chemical reduction in the presence of ammonia. The generalized scheme of this chemistry is shown in Fig 1.4. The secondary amines are formed by reductive amination of the aldehydes and ketones in the presence of primary amines. The generalized scheme of this chemistry is shown in Fig 1.5.

The synthesis of NPPB is achieved by reductive amination of hydrocinnamaldehyde as the aldehyde, with 2-amino-5-nitrobenzoic acid as the primary amine (Fig 1.6). The reducing agent selected for this reaction is sodium cyanoborohydride (NaBH_3CN), which reduces a wide variety of functional groups with remarkable selectivity. The use of NaBH_3CN as the reducing agent in reductive amination was established by the Borch group (51). This group found that NaBH_3CN could reduce enamines under certain conditions, for example when the salt was formed by protonation at an appropriate pH. The protonation of the enamine group forms the readily reducible iminium salt, which is reduced by the cyanohydridoborate anion to convert the salt to the tertiary amine. The group also revealed that a pH of 6-7 was suitable in providing the iminium salt but the reduction of aldehydes and ketones was negligible in this pH range. When the hydrocinnamaldehyde is treated with the 5-nitroanthranilic acid, the iminium group is formed from a carbonyl group on the hydrocinnamaldehyde and an amine group on the 5-nitroanthranilic acid. The initial step is unfavourable, but the optimum pH for the iminium salt formation from the aldehydes and ketones treated with the amines, is pH 6-7.

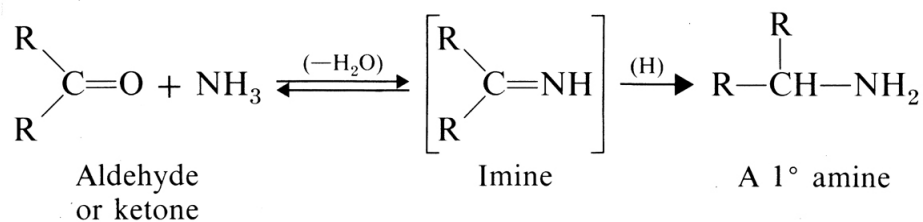


Figure 1.4 Generalized scheme of reductive amination. Aldehydes and Ketones are converted to the primary amines, in the presence of ammonia.

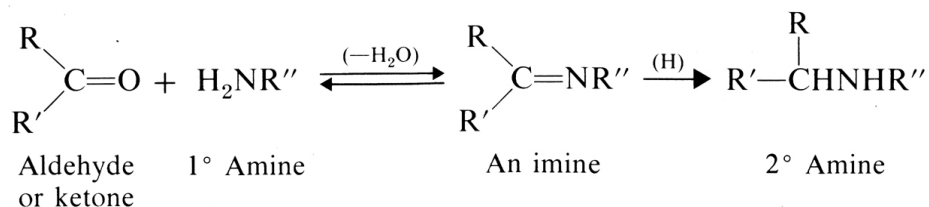


Figure 1.5 Generalised scheme of reductive amination to form secondary amine. Aldehydes and Ketones are converted to the secondary amines, in the presence of primary amine.

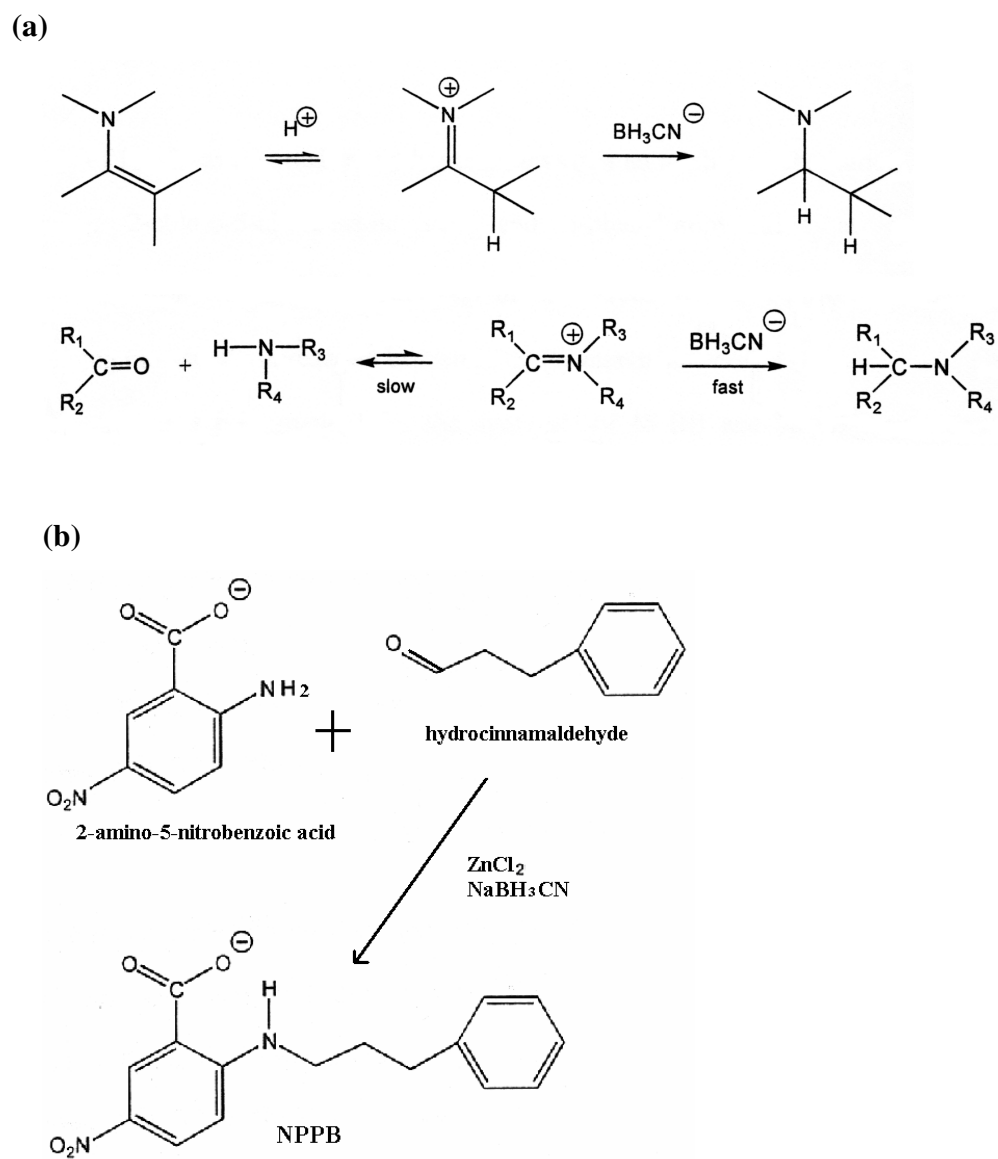


Figure 1.6 NPPB synthesis

(a) General scheme of reductive amination catalysed by cyanohydridoborate anion. The imminium salt formed by protonation is trapped by cyanohydridoborate anion to form tertiary amine.

(b) Summary of NPPB synthesis.

Even though the reduction step is unfavourable in this pH range, the formed imminium salt is trapped immediately by NaBH_3CN , and then reduced to form NPPB. This method of reductive amination can be improved with a Lewis acid catalyst. In this research, zinc chloride (ZnCl_2) is used as a Lewis acid catalyst, which can help improve yields of imminium intermediate formation (50). Use of titanium(IV)isopropoxide ($\text{Ti}(\text{OiPr})_4$) as the Lewis acid catalyst also can improve yields if the formation of the imminium intermediate proves difficult (52).

Importantly the use of different aldehydes and amines in the above reactions allows the synthesis of a variety of NPPB analogues. In this thesis three such analogues 2-(3-phenylpropylamino) benzoic acid (PPAB), 5-nitro-2-heptylamino benzoic acid (HANB) and 2-nitro-5-heptylamino benzoic acid (HANB-2) were of interest. The synthesis of PPAB is achieved by reductive amination of hydrocinnamaldehyde as the aldehyde, with 2-aminobenzoic acid as the primary amine (Fig 1.7). This NPPB analogue has no nitro-group on the 5th position of the benzene ring and thus enables investigation of the importance of the nitro-group for the inhibitory action of NPPB.

The starting materials in the synthesis of HANB are heptaldehyde as the aldehyde and 2-amino-5-nitrobenzoic acid as the primary amine (Fig 1.8). This analogue is lacking the benzene ring and thus enables investigation of the role of the benzene ring at the end of the hydrocarbon chain on inhibitory actions.

The starting materials of HANB-2 are heptaldehyde as the aldehyde and 5-amino-2-nitrobenzoic acid as the primary amine (Fig 1.9). The position of carboxyl-group is shifted in this analogue relative to HANB.

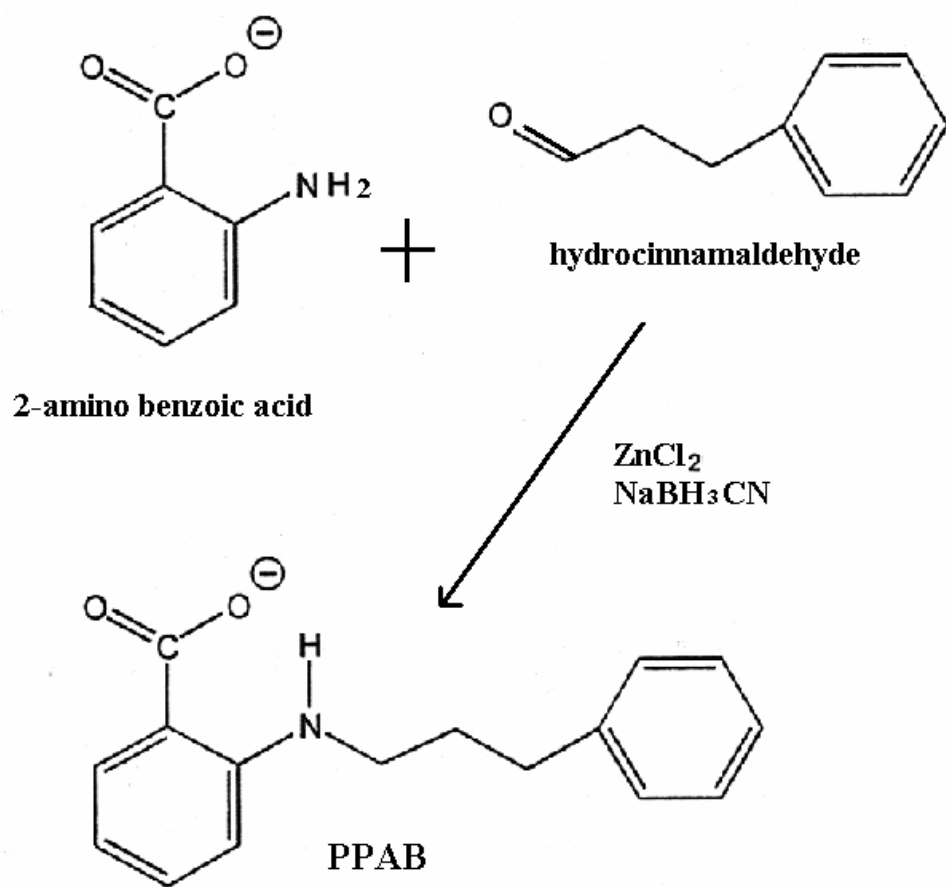


Figure 1.7 PPAB synthesis

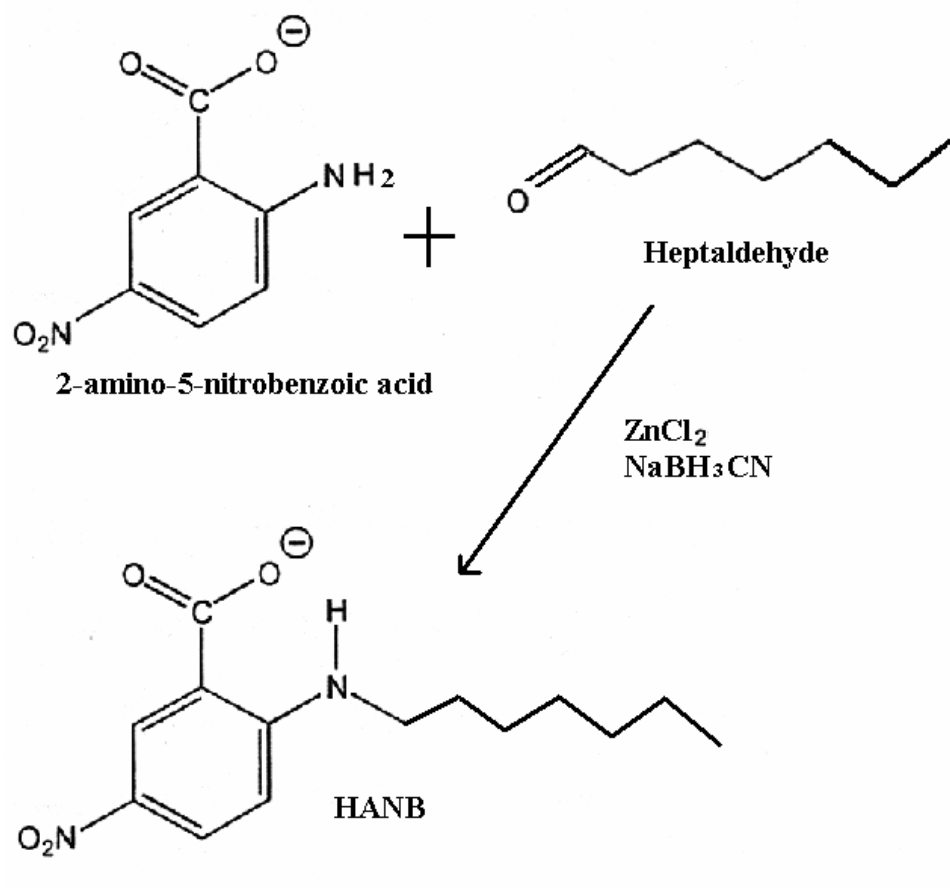


Figure 1.8 HANB syntheses.

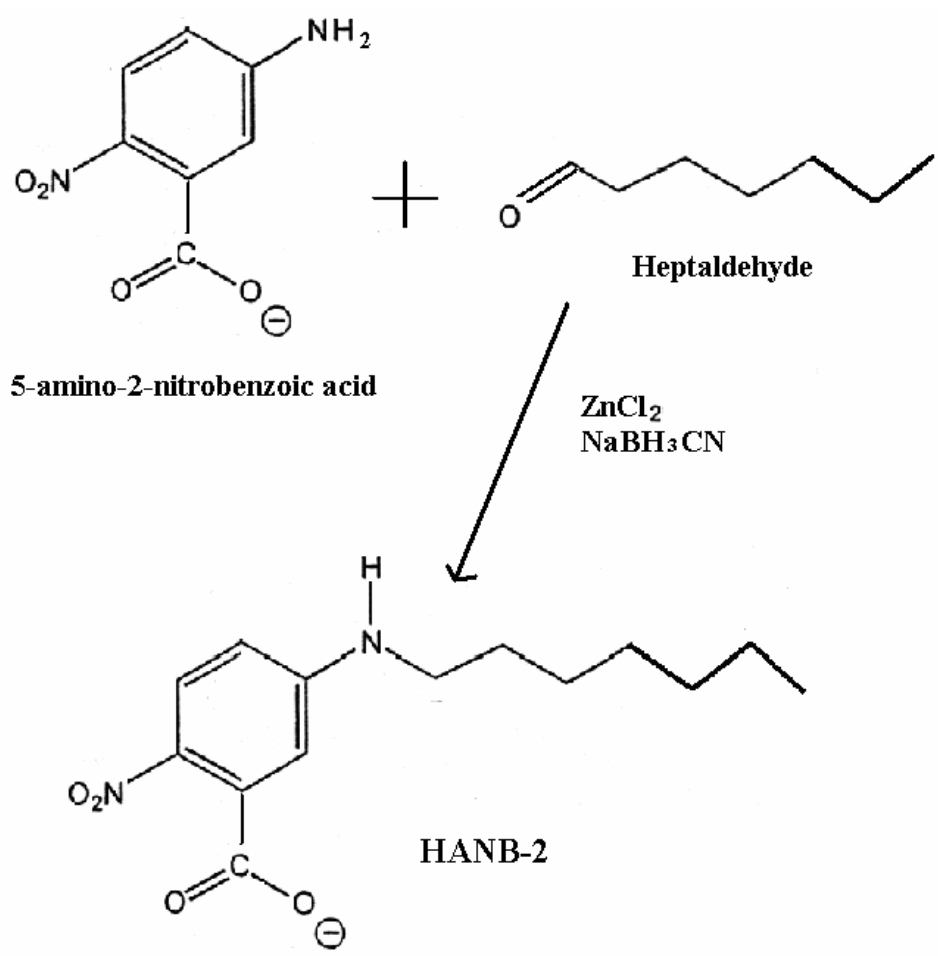


Figure 1.9 HANB-2 syntheses.

1.5.2 Cytoplasmic Streaming

Cytoplasmic streaming is the circular flow of cytoplasm, with the coordinated movement of particles, vacuoles, and other organelles through the cytosol. It provides a means of speeding up movement of molecules throughout large plant cells that would otherwise be reliant upon simple diffusion for their movement from one side of a cell to the other. This process has been reported in a variety of cell types. In large plant cells, such as *Chara* and *Nitella*, cytoplasmic streaming can be observed easily under the microscope. The movement occurs in a circular path down one side of a cell and then back up the other side. The rate of cytoplasmic streaming can be identified by observation of movement of one particular particle under the microscope with an eyepiece micrometer. The rate of streaming is sensitive to changes in ion concentrations and ion fluxes between the inside and the outside of the cell. The cessation of cytoplasmic streaming caused by an increase of the cytoplasmic Ca^{2+} level has been reported (53). Because cytoplasmic streaming is sensitive to the ion fluxes, it is also affected by the presence of ion channel inhibitors. Observation of any changes in the cytoplasmic streaming rate with the presence of ion channel inhibitors can thus be used as an indirect measure of their inhibitory effect. The effect of NPPB and its analogues on cytoplasmic streaming in *Nitella hookeri* has been reported and their IC_{50} values have been stated (54). The study of ion channel inhibitors on cytoplasmic streaming does not however provide direct information on the mode of action of the inhibitors. However, since inhibitory effects of NPPB and its analogues on cytoplasmic streaming have been reported, this model can be exploited as a simple preliminary assay for studying the effects of structural modification. In this report, NPPB purchased from Sigma Chemicals was tested on cytoplasmic streaming in *Nitella hookeri*, while the existing literature used synthesised NPPB, to

confirm the significance of this study model.

1.5.3 Turgor Regulation

Plants maintain higher concentrations of solutes in their cells than the external media, thus water tends to flow into the cytoplasm and the cells swell. However, the continued enlargement of the cells is prevented by the rigid cell walls. As result, the cells build up the large positive internal hydrostatic pressure, called turgor pressure. At this point, the cells are so called turgid, which is very firm, and this is the preferred healthy state for most plant cells.

There are three main roles of turgor in plant and algae cells (55). In the early stages of the development of plants and algae, when they have not yet established structural elements in the vascular system, the major function of turgor is to maintain the shape and rigidity of plant and algae cells and tissues. An example of when this process goes wrong is the phenomena of wilting in plants that are severely water stressed.

Turgor regulation also plays a major controlling role in growth and cell expansion. Since water uptake for cell growth is a passive phenomenon, the difference in water potential across the membrane is the driving force of water absorption. This water potential is stated from osmotic pressure and turgor pressure. Thus, the relative growth rate of the cells depends on the relative hydraulic conductance, which is a measure of the relative ease with which water can enter the cell, the osmotic pressure, and the turgor pressure. When the cell growth is stated as cell wall expansion, the cell wall relaxation and expansion also depend on turgor pressure. Also turgor regulation measurements in saprophytic hyphal organisms suggest that turgor may be the one of the multiple mechanisms of hyphal growth (56,57).

Moreover, turgor changes have an important role in rapid and reversible movements in response to various stimuli, such as stomatal opening and closing, rapid leaf movements of *Mimosa* and sleep movement of bean plants. The sleep movement is characterized by the lowering of the leaves in the evening and raising them to a horizontal position in the morning. These movements are deeply related to the ion flux (especially K^+) across the membrane.

In plants and algae, changes in turgor are caused by the transport of solutes, such as ion flux into or out of cells. This movement of solutes across the membrane establishes an osmotic gradient, which facilitates a corresponding movement of water in or out of the cells (depending on the direction of the gradient). Thus, any change in turgor pressure is likely to be indicative of the activity of ion channels, which will regulate the osmotic gradient.

In this report, the turgor pressure of internodal cells of *Nitella hookeri* was measured by using a pressure probe. The turgor regulation of the internodal cells in hyperosmotic solution was observed as the control. Using this control, the effect of ion channel inhibitors, such as NPPB and PPAB, in the turgor regulation of the internodal cells bathing in the hyperosmotic solution was observed.

1.5.4 Aequorin Technology

Calcium ions are now firmly recognised as playing a crucially important role in several plant signalling pathways. For example early pharmacological and $^{45}Ca^{2+}$ based studies concluded that the activation of plant defence response depends on the Ca^{2+} influx from apoplast into the cytosol leading to the increases in cytosolic free Ca^{2+} in the plant cells. As such techniques that

enable measurement of Ca^{2+} or the ability to track changes in Ca^{2+} concentration are of great interest and importance.

There are several techniques for monitoring the intracellular Ca^{2+} homeostasis, but they all have advantages and disadvantages. Ca^{2+} sensitive dyes have been used to monitor the cytosolic Ca^{2+} level during interaction of pathogens with plant cells (58). However, many problems can be encountered with fluorescent probes, such as the difficulty in getting them inside the plant cell of interest, their buffering capacity or toxicity, and a limited application. The most popular technique, nowadays, for the calcium signalling studies is aequorin technology, which is based on bioluminescence.

Aequorin is a calcium sensitive luminescent protein found in jelly fish, and it is composed of an apoprotein (apoaequorin), which is a polypeptide of relative molecular mass $\sim 22\text{kDa}$, and a prosthetic group consisting of a luciferin molecule called coelenterazine. The mechanism of Ca^{2+} detection using aequorin is depicted in Fig 1.10. Basically the hydrophobic luminophore coelenterazine enters the cytosol, and spontaneously binds with apoaequorin in the presence of molecular oxygen, this gives rise to the formation of holoaequorin. The binding of three Ca^{2+} ions per molecule triggers a conformational change and dissociation of apoaequorin. This causes the coelenterazine to be oxidised to coelenteramide, with CO_2 production and importantly the emission of blue light ($h\nu=468\text{nm}$) which can be detected with a luminometer.

The aequorin can be introduced to large plant cells by microinjection. However, the aequorin is also able to be introduced into plant cells using a

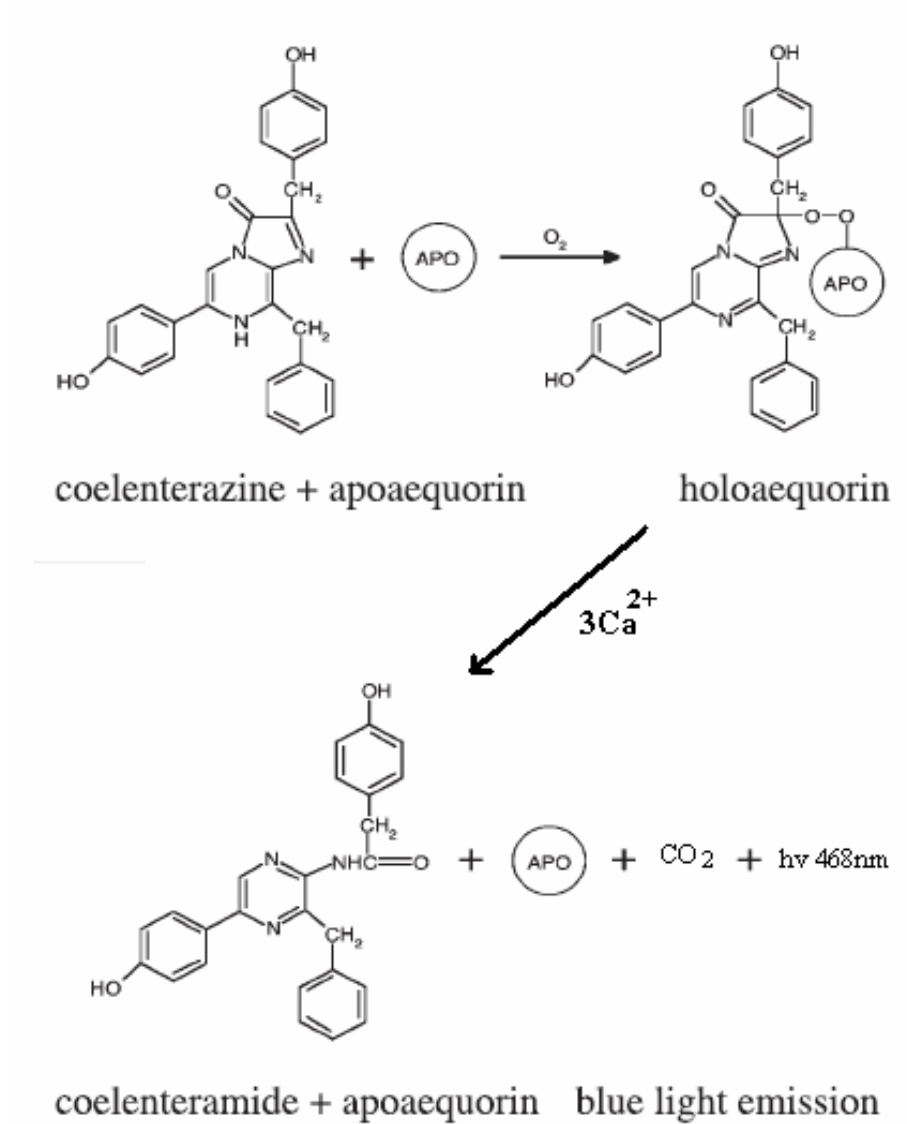


Figure 1.10 Mechanism of light emission by aequorin upon Ca²⁺ binding.

stable transformation technique. The probe can be stably expressed not only in the cytoplasm, but also targeted to different organelles, subcellular compartments or tissues by appropriate targeting of signal sequences or fusion constructs. A diagram of the targeting aequorin into plants cell is shown in Fig 1.11. This transgenic aequorin approach allows monitoring of any change of Ca^{2+} levels in response to touch, cold shock, and pathogenic elicitors (59).

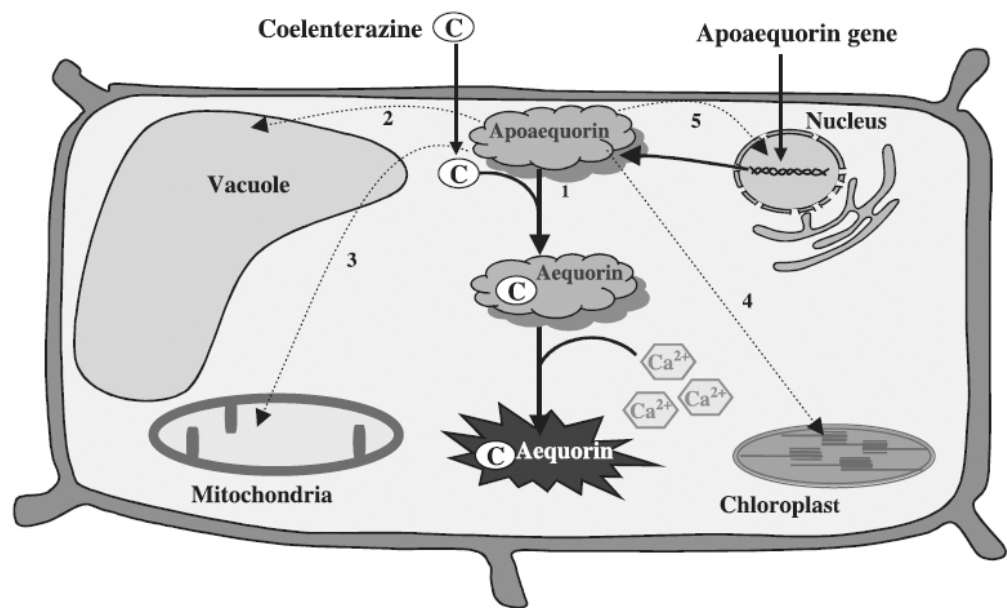


Figure 1.11 Targeting aequorin into plant cells. (Adapted from (60))

Chapter 2 Material and Methods

2.1 Sample Collection

Samples of *Nitella hookeri* was collected from the Okeover stream and Avon River that both flow through the University of Canterbury campus in Christchurch New Zealand. The dense population that were found under shaded areas of the stream and river were used for collection. The sample was caught by a long hook and collected in a bucket with plenty of water also from the stream. Using another bucket of water, the large debris, soil, and other organisms were removed. The sample was transferred to a fish tank (18x38cm) with the water from the stream. The tank was covered by foil to avoid direct sunlight and create similar environment as their natural habitat. The water was continuously aerated.

2.2 Chemical Synthesis

2.2.1 NPPB

The synthesis of NPPB was achieved by reductive amination of hydrocinnamaldehyde as the aldehyde, with 2-amino-5-nitrobenzoic acid, which is also called 5-nitroanthranilic acid, as the primary amine. The purity of the starting materials, which were obtained from Aldrich chemicals, was assessed by ¹H NMR and thin layer chromatography (TLC). Because the TLC result showed some impurity, the hydrocinnamaldehyde was purified in the lab by distillation. After purifying the starting materials, the reaction was started by dissolving 2-amino-5-nitrobenzoic acid (1g, 5.49mmol) and hydrocinnamaldehyde (1.089ml, 8.25mmol) in super dry methanol (10~20ml) in a 100ml round-bottom flask under a drying tube. The mixture

was stirred at room temperature for 2 hours.

According to the TLC of the crude product, some remains of amine were confirmed. Therefore, to achieve higher yields, an excess of aldehyde was added. The reaction was carried by the amine and aldehyde with a ratio of 1:1.5mol, rather than 1:1mol

The super dry methanol was prepared by the method established by Lund and Bjerrum (61). A mixture of magnesium turnings (5g), iodine (0.5g) and 50ml of absolute methanol was warmed up until the colour of the iodine disappeared. Up to 1L of methanol was added and refluxed for 2~3 hours. The super dry methanol was distilled off and collected to the flask containing molecular sieves with a rubber cap on. The transfer of the super dry methanol was done using a syringe under nitrogen gas streaming.

While stirring the aldehyde/amine mixture, a suspension of sodium cyanoborohydride (NaBH_3CN , 0.69g, 10.98mmol) and zinc chloride (ZnCl_2 , 0.75g, 5.49mmol) in super dry methanol (10~20ml) was also stirred at room temperature for 2 hours, in a 100ml round-bottom flask under a drying tube.

After 2 hours stirring, the reducing agent mixture ($\text{NaBH}_3\text{CN}/\text{ZnCl}_2$) was added to the aldehyde/amine mixture. The reaction was carried out by stirring at room temperature for 20 hours.

After this time, the solution was concentrated *in vacuo* on a rotary evaporator. The crude product was then dissolved in ethyl acetate and hydrochloric acid (HCl, 3M). The addition of HCl makes the product soluble in the organic phase by protonation of the carboxylate group of NPPB. The

organic phase was collected in the flask, then the aqueous phase was washed using brine (aqueous saturated NaCl), which moved the product into the aqueous layer by forming the salt of NPPB. Further washing by HCl returned the product into the organic phase. After collecting the organic phase, the aqueous phase was back washed with ethyl acetate. All fractions of organic phase were collected into a conical flask, and magnesium sulphate (MgSO_4) was added to remove any residual water. The MgSO_4 was removed by filtration, and then the filtrate of the dried solution was concentrated *in vacuo*. The crude product had a bright yellow colour.

A small amount of crude product was dissolved in the ethyl acetate for TLC using 30% ethyl acetate/ petroleum ether. The starting materials, which were hydrocinnamaldehyde and 2-amino-5-nitrobenzoic acid, were compared with the crude product by TLC. The product eluted as two spots on the silica plate with one of them more concentrated and the other showed the same spot of 2-amino-5-nitrobenzoic acid under UV light.

The crude product was purified by column chromatography and recrystallization. The existing literature suggests the use of column chromatography to purify NPPB (50). The column was made with silica gel 60 using the ethyl acetate / petroleum ether solvent as elutant. Because NPPB is not soluble, the product was dissolved in the ethyl acetate, first. Then silica gel was added. The mixture was concentrated *in vacuo* on a rotary evaporator using tissue paper to stop dried silica gel getting into the system. The silica gel which NPPB stuck to was gently poured into the top of the column. The 30% ethyl acetate / petroleum ether solvent was used as elutant first, this was then changed to the 40% and the 50% solvents, while collecting the fractions. TLC was performed on each fraction. The fractions which showed same spot

on the silica plate were combined and concentrated *in vacuo* on a rotary evaporator.

However the column chromatography was not efficient in the purification of NPPB, regardless of whether long or short columns with a vacuum were used. During the purification with column chromatography, NPPB tended to decompose. To remove impurities, the column had to be run several times to collect pure NPPB, consequently it showed a low yield.

The re-crystallization methodology showed a higher yield of pure product than the column chromatography. Two types of solvents were tested in order to remove impurities from the NPPB. The crude product was dissolved with a minimum amount of methanol or ethyl acetate. Water or petroleum ether was added drop wise to the suspension until it just formed a crystal. Even though the crude product was hard to dissolve in methanol and required heat to be dissolved, the use of methanol / water led to the formation of much better crystals than ethyl acetate / petroleum ether. The crystal was filtered off, and then the purity of synthesized NPPB was assessed by TLC and ¹H NMR (500MHz, CDCl₃ as solvent).

2.2.2 PPAB

The synthesis of PPAB was achieved by reductive amination of hydrocinnamaldehyde as the aldehyde, with 2-aminobenzoic acid, which is also called anthranilic acid, as the primary amine. The reaction was started by dissolving 2-aminobenzoic acid (1g, 7.29mmol) and the distilled hydrocinnamaldehyde (1.443ml, 10.94mmol) in super dry methanol (10~20ml) in a 100ml round-bottom flask under a drying tube. Same as for NPPB, the mixture was stirred at room temperature for 2 hours. While

stirring the aldehyde/amine mixture, a suspension of NaBH₃CN (0.92g, 14.58mmol) and ZnCl₂ (0.99g, 7.29mmol) in super dry methanol (10~20ml) was also stirred at room temperature for 2 hours. After 2 hours stirring, the reducing agent mixture (NaBH₃CN/ ZnCl₂) was added to the aldehyde/amine mixture. The reaction was carried out by stirring at room temperature for 20 hours. The crude product was extracted using aqueous saturated NaCl and HCl, the same as for NPPB. The suspension was washed until the purple/pinkish colour disappeared; this led to the achievement of higher yields.

Unlike NPPB, PPAB could be purified satisfactorily by column chromatography. The column was made with silica gel 60 using the 20% and 30% ethyl acetate / petroleum ether solvent as elutant. TLC was used to assess the purity of the fractions. It showed a high yield of pure product after the column chromatography. For further purification, the re-crystallization with methanol / water was used. Use of a minimum amount of water and leaving the suspension over night in a fridge led to higher yields. The purity of synthesized PPAB was assessed by TLC and ¹H NMR (500MHz, CDCl₃ as solvent).

2.2.3 HANB

The synthesis of HANB was achieved by reductive amination of heptaldehyde, which is also called heptanal as the aldehyde, with 2-amino-5-nitrobenzoic acid as the primary amine. The procedure was carried out the same as for NPPB, 2-amino-5-nitrobenzoic acid (1g, 5.49mmol) was dissolved with the distilled heptaldehyde (1.11ml, 8.25mmol) in super dry methanol (10~20ml). The reducing agent suspension was made by dissolving NaBH₃CN (0.69g, 10.98mmol) and ZnCl₂ (0.75g, 5.49mmol) in super dry

methanol (10~20ml) and was stirred for 2 hours. The reaction was started by adding the reducing agent mixture ($\text{NaBH}_3\text{CN}/\text{ZnCl}_2$) to the aldehyde/amine mixture, and then it was stirred at room temperature for 20 hours. Same as for NPPB, the crude product was extracted using aqueous saturated NaCl and HCl.

HANB could also be purified by the column chromatography efficiently. As for PPAB, the column was made with silica gel 60 using the 20% and 30% ethyl acetate / petroleum ether solvent as elutant. HANB was purified by both the long silica gel column and also using a radial disk of silica gel, called chromatatron.

After the chromatography, a high yield of pure product in the fractions was identified by the TLC. For further purification, the product was re-crystallized with methanol and minimum amount of water. The crystallized product was filtered after leaving over night in the fridge. The purity of synthesized HANB was assessed by TLC and ^1H NMR (500MHz, CDCl_3 as solvent).

2.2.4 HANB-2

This is the first synthesis of HANB-2, which reverses effectiveness of the reductive amination method for synthesizing a large variety of NPPB analogues. The synthesis of HANB-2 is achieved by reductive amination of heptaldehyde as the aldehyde, with 5-amino-2-nitrobenzoic acid as the primary amine. Because the molecular weight of amines used for HANB and HANB-2 were identical, the aldehyde/amine and the reducing agent mixture were prepared the same as for HANB. However, the amount of starting material was doubled for this synthesis. Therefore, 5-amino-2-nitrobenzoic

acid (2g, 10.98mmol) and the distilled heptaldehyde (2.21ml, 16.47mmol) were dissolved in the super dry methanol as the aldehyde/amine mixture. The reducing agent suspension was made by dissolving NaBH₃CN (1.38g, 21.96mmol) and ZnCl₂ (1.50g, 10.98mmol) in super dry methanol. As for NPPB, the reaction was carried out by stirring at room temperature for 20 hours, and then the crude product was extracted by aqueous saturated NaCl and HCl.

The purification of HANB-2 was much more difficult than for the other compounds. The product did not form crystals, so re-crystallization was not an option to purify HANB-2. Column chromatography and radical silica chromatography performed on chromatatron were used to remove impurities. The purity of fractions was assessed by TLC, and then the presence of the desired product was assessed by ¹H NMR. The column chromatography was run several times with different solvents, such as 30%, 40% of ethyl acetate / petroleum ether, 50% of ether / petroleum ether, and 100% ether. The purity of synthesized HANB-2 was assessed by TLC, ¹H NMR (500MHz, CDCl₃ as solvent), ¹³C NMR, mass spectra (MS) and infrared spectra (IR).

2.3 Cytoplasmic Streaming

2.3.1 Sample Preparation

Nitella hookeri was collected from the Okeover stream and kept in the aerated fish tank in the lab as described above. The sample was allowed to settle in the fish tank, typically for several days, before any experiment.

For streaming experiments, the previously published study (54) suggested using a slide chamber. The internodal cells were placed onto a slide chamber

filled with adequate solution to submerge the cells. The slide chamber was prepared from a microscope slide glass with a hole drilled in the middle. One side of the slide chamber was sealed by sticking a cover slip using Vaseline. The bathing solutions containing inhibitors were applied into the slide chamber by perfusion. However, it was found that the slide chamber was too thick to be used under the microscope using a 40x objective, which was needed to provide adequate resolution to observe streaming with the greatest accuracy. Therefore, in this report, the internodal cells were prepared onto a slide glass with white “twink” on the four corners of cover slip to enable sufficient space for bathing cells. Also, because of difficulty of perfusion to change the bathing solutions, the internodal cells were at the time bathed in 10ml of each solution in an upturned petridish lid.

2.3.2 Streaming Rate Measurement

Streaming rates were determined by recording the velocities of individual particles or organelles, as observed using a 40x objective under an Olympus BH2 microscope with an eyepiece micrometer. Time was measured when a particle moved certain distance on the eyepiece micrometer. Using a slide micrometer, the distance on the eyepiece micrometer was determined. In this experiment, one bar of the eyepiece micrometer was 2.8 μ m.

Cytoplasmic streaming is sensitive to physical stimuli, such as light and touch, both of which can induce Ca²⁺ fluxes and action potentials. Therefore, the cells were placed into the petridish containing 10ml of artificial pond water (APW) and left for 15 minutes before measurement. The APW contained 1mM NaCl, 0.1mM CaCl₂, 0.1mM KCl and was adjusted to pH 8 or pH 10 with KOH. After determining the initial streaming rate in APW, the internodal cells were placed into the petridish lid with 10ml of APW containing the

desired concentration of inhibitor. The effect of inhibitors on cytoplasmic streaming was determined by measuring the streaming rate at 5 minutes and 10 minutes after the cells were placed into the inhibitor solution. After streaming rate measurement in the presence of inhibitors, the internodal cells were again placed into the petridish lid with 10ml of APW (minus the inhibitor) to observe the recovery of cytoplasmic streaming in the absence of the inhibitor. The streaming rate was determined after 10 and 20 minutes after the cells were reimmersed in APW. For each inhibitor concentration, 10 internodal cells were assayed, and for each of these cells, the velocities of 5 particles were measured.

Because stock solutions of inhibitors were prepared within ethanol, the effect of ethanol on streaming should be considered. Control experiments were carried out that measured the effect on streaming of the highest concentration of ethanol (1% v/v) that the cells were exposed to during the inhibitors experiments (54). This was found to have no effect on streaming rate, and in fact most of the inhibitor solution contained less than 1% (v/v) of ethanol. In this report, the effect of NPPB and niflumic acid on cytoplasmic streaming rate was determined. Both chemicals were purchased from Sigma Chemicals and NPPB was prepared in pH 8 and pH 10 APW, and the niflumic acid was prepared in pH 8 APW.

2.4 Turgor Regulation

2.4.1 Sample Preparation

Nitella hookeri was collected from the stream and kept in the aerated fish tank in the lab as described above. The sample was allowed to settle in the fish tank, typically for several days, before the experiment.

For the turgor regulation experiment, a few internodal cells were collected from the fish tank then blotted gently onto a paper towel. The sample was then placed onto a small petridish. Individual filaments were separated and stuck onto the petridish using small pieces of adhesive tape. The tape was put onto the cell which was next to the cell used for the measurement to minimise physical damage of those cells from which measurements were made. This holding of sample cells makes it easier to impale the microcapillary into the cell. The sample cells were placed onto the petridishes as quickly as possible to minimise disruption.

Immediately, 7ml of artificial pond water (APW) or hyperosmotic solution with/without inhibitors were poured into the petridish to cover the sample cells. They were left more than 30min to recover before the measurement. The APW contained 1mM NaCl, 0.1mM CaCl₂, 0.1mM KCl and was adjusted to pH8 with KOH. The hyperosmotic solution comprised the relevant concentration of D-sorbitol (SIGMA) made up in APW. The inhibitors tested in the turgor regulation experiments were NPPB and PPAB.

2.4.2 Pressure Probe Measurements

A pressure probe is a device for direct measurement of the cell turgor, developed by Zimmermann in 1969 (Fig 2.1). The microcapillary was made from borosilicate capillary (1.2mmOD, 0.69mmID, Harvard Apparatus GC120-15, Kent, UK). The borosilicate capillary was constructed using a Narashige puller (Model PC-10, Narashige, Tokyo, Japan). Basically the wire around the capillary was heated up, while the weight attach to the capillary stretched the glass forming a microcapillary, which had fine sharp pointy end. The microcapillaries were filled with low viscosity silicone oil

(WACKER AS4, Wacker-Chemie, Munchen, Germany). The silicone oil was applied to the microcapillary by a syringe with a capillary tube attached. The microcapillary has to be totally filled with silicon oil. Any bubbles in the microcapillary were removed by gentle (and sometimes extensive) tapping. The quality of the tip of the microcapillary was checked under the microscope. The prepared microcapillaries were kept in the petridish to avoid dust, and placed on Blu-tac to prevent breakage of sharp end.

Before the microcapillary was attached to the pressure probe, the metal rod that was used to increase/decrease pressure was pulled back to the end of the pressure probe. The microcapillary was attached to the screw cap with a rubber seal attached to the other end of the microcapillary. The chamber of the pressure probe was filled with the silicon oil. The microcapillary was attached to the pressure probe by tightening the screw cap. Prior to experiments a check was made to see if any air bubbles were present in the chamber and the microcapillary. If any bubbles were present the microcapillary was discarded and a new one was attached. The presence of bubbles can lead to erroneous turgor values.

The pressure probe was attached to a manipulator and the sample in the petridish was observed under an inverted microscope. First, the sample cells were checked to confirm the presence of cytoplasmic streaming. If streaming was present the manipulator was used to bring the microcapillary into the sight of the objective lens. When the microcapillary was first immersed in solution, surface tension may pull the solution into the microcapillary tip. In such cases pressure was slowly applied to push the silicon oil/bathing solution interface back to the end of the microcapillary tip.

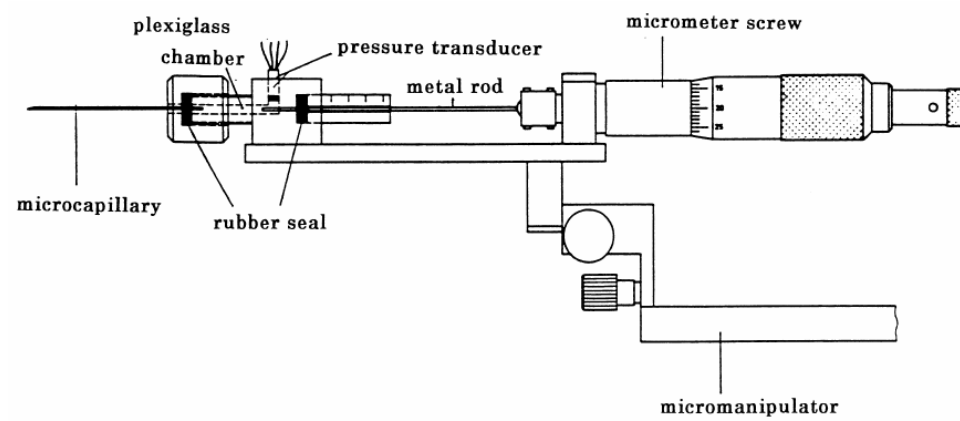


Figure 2.1 Pressure probe for turgor pressure measurement.

The microcapillary was gently impaled into the sample cell. Typically with a successful impalement, the cytoplasm/oil interface was forced back into the microcapillary due to turgor pressure. At this point, the pressure measured by the pressure transducer was recorded. Pressure was then slowly applied using the metal rod in the pressure probe chamber until the meniscus was pushed back to the microcapillary tip. When the meniscus reached to the tip, the pressure was again recorded. The difference between the pressure at the point when the meniscus was drawn back and the pressure when it was pushed back to the tip using the rod was calculated and taken as a measure of the turgor pressure of the sample cell.

2.4.3 Test Solutions

The hyperosmotic solution was made by addition of D-sorbitol (SIGMA) to the APW. The sample cells tended to lose rigidity in higher concentrations of hyperosmotic solution. Consequently, this made it difficult to impale the microcapillary into the cells. Several different concentration of hyperosmotic solutions were tested for the pressure probe measurement. In this research, the APW containing 100mM of sorbitol was used as the hyperosmotic solution, which is the highest concentration to be able to work with pressure probe measurement.

For the inhibitor experiments with NPPB, hyperosmotic solutions containing 100, 50 and 25 μ M of NPPB were used. The hyperosmotic solution containing 100 μ M of NPPB was the highest concentration of inhibitor, which did not terminate cytoplasmic streaming of the sample cells.

The concentration of the PPAB solutions used for the experiment was 500, 250, and 50 μ M of PPAB. Because of insolubility of PPAB, the pH of the

hyperosmotic solution was adjusted from pH 8 to pH 10. The PPAB was dissolved in ethanol as the stock solution, and the stock solution could be dissolved in hyperosmotic solution with a pH of 10. The turgor pressure of the sample cells in pH 8 and pH 10 of hyperosmotic solution were obtained to confirm that there was no significant effect of pH of the solution to the pressure probe measurement.

2.4.4 Osmotic Potential

Osmotic pressure is the hydrostatic pressure, which causes the influx of water from low solute concentration to the high solute concentration, through a semipermeable membrane. Strictly speaking, the isolated solution has no osmotic pressure, but has osmotic potential which can be calculated from osmolality of the solution. The Osmolality is an expression of the total concentration of dissolved particles in a solution without regard for the particle size, density, configuration, or electrical charge. The osmolality of the solutions used for the turgor regulation experiment was measured by an osmometer (5500 Vapor Pressure Osmometer, Wescor). The osmotic potential was calculated by following equation:

$$\pi = CRT$$

Where π is osmotic potential (MPa), C is osmolality (Os mol/kg), R is the universal gas constant (0.00831 MPa/Os mol/kg/K), and T is the absolute temperature (293K).

In the plant cells, water tends to flow into the cytoplasm, but the enlargement of the cells is prevented by the rigid cell walls. As result, the cells build up the large positive internal hydrostatic pressure, called turgor pressure. Because the turgor pressure is established by the osmotic pressure,

the osmotic potential of each test solution should be consider for comparing the effect of test solutions toward turgor pressure of the sample cells.

2.5 Cytosolic Free Calcium Analysis

2.5.1 Aequorin Transformed Cells

Nicotiana plumbaginifolia plants (generated from line MAQ2.4 transgenic plants) expressing apoaequorin were used to generate dark grown cell suspensions (62). The leaves grown from the transgenic seeds were treated and transferred to W-38 agar to promote callus formation. The calli were fragmented, transferred to liquid W-38 medium, and maintained in suspension by continuous shaking. The *Nicotiana plumbaginifolia* aequorin transformed cells were obtained from the team of A.Pugin (63) and the transformed line of tobacco was furnished by MR.Knight (59). Every 8 days, 8ml of aequorin transformed cells were transferred to 100ml of fresh liquid Chandler's medium (64), and maintained in a dark grown suspension by continuous shaking.

Before reconstitution of aequorin and exposure to the channel inhibitors, such as NPPB, PPAB and HANB, 8 day-old transgenic cell suspensions were collected and washed by filtration with a suspension buffer containing mannitol (175mM), CaCl₂ (0.5mM), K₂SO₄ (0.5mM), and Hepes (2mM, adjusted to pH 5.75). They were resuspended in suspension buffer to give a final concentration of 0.1g fresh weight/ml. *In vivo* reconstitution of aequorin was carried out by adding 2μL of coelenterazine (5mM stock solution in methanol) to 10ml of cell suspension for at least 3 hours in the dark.

The vital dye neutral red was used to test for cell viability (65).

Accumulation of the neutral red within the vacuole was observed by light microscopy. Cells that lost membrane integrity and did not stain with neutral red were considered unviable and were discarded. A 1mL aliquot of cells was washed with 1mL of a solution containing mannitol (175mM), CaCl₂ (0.5mM), K₂SO₄ (0.5mM), and Hepes (2mM adjusted to pH 7.0), and then incubated for 5min in the same solution to which was added the neutral red to give a final concentration of 0.01% (w/v). At least 500 cells were examined for each experiment and three independent experiments were performed for each treatment.

2.5.2 Luminescence Measurements

Luminescence measurements were made using a digital luminometer (Lumat LB9507; Berthold, Bad Wildbad, Germany). Coelenterazine-treated culture aliquots (250µL) were transferred to a luminometer glass tube. Luminescence was measured every second for the duration of the experiment as relative light units per second. The recordings were exported simultaneously into Excel on a computer. All inhibitors and control solvents were added at 15 min before cold-shock treatments. At the end of the experiment, all of the unconsumed aequorin was discharged by injecting 300µl of a lysis buffer solution of 2% Nonidet P-40, 10 mM CaCl₂ and 10% ethanol into the luminometer glass tube to determine the total light output.

The quantitation of intracellular Ca²⁺ concentration was obtained by transforming data of each luminescence curve using the equation described by Allen *et al* (66),

$$[Ca^{2+}] = \{(L_0/L_{max})^{1/3} + [K_{TR}(L_0/L_{max})^{1/3}] - 1\} / \{K_R - [K_R(L_0/L_{max})^{1/3}]\}$$

Where L is the amount of light per second, L_{max} is the total amount of light present in the entire sample over the course of the experiment, $[Ca^{2+}]$ is the

calculated Ca^{2+} concentration, K_{R} is the dissociation constant for the first Ca^{2+} ion to bind, and K_{TR} is the binding constant of the second Ca^{2+} ion to bind to aequorin. For the native coelenterazine and the specific aequorin isoforms, which were used in these experiments at 22°C , a value of $K_{\text{R}} = 2 \times 10^6 \text{ M}^{-1}$ and $K_{\text{TR}} = 55 \text{ M}^{-1}$ was used (67).

Chapter 3 Results

3.1 Chemical Synthesis

3.1.1 NPPB

The crude product after extraction with the aqueous saturated NaCl and HCl was a bright yellow colour. The re-crystallization of the crude product also formed the bright yellow crystals. Although the existing literature suggests the use of column chromatography to purify NPPB (50), the product tends to decompose during the chromatography. After the first chromatography, the crude product still showed the presence of impurities on the TLC. To remove the impurities, the column chromatography had to be run several times, consequently it lowered the total yield.

Almost all of the impurities were removed by the one step of re-crystallization with methanol and water. However, the product still remained in the filtrate, so the re-crystallization was performed three times for each filtrate. The final product was assessed its purity by TLC and ^1H NMR.

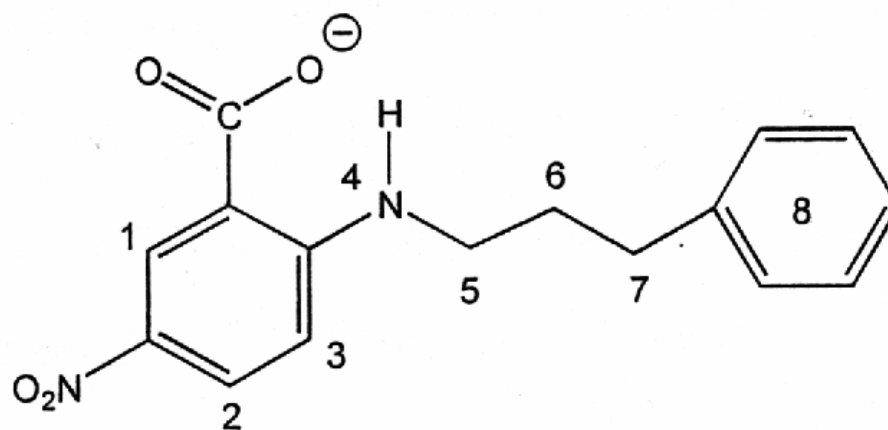
As regards TLC, there was only one spot with an R_f value of 0.35, which is relative to the spot of NPPB from Sigma Chemicals using the 30% ethyl acetate / petroleum ether as elutant. This inferred that the all impurities were removed.

The ^1H NMR was run to ensure the final product was NPPB. Nuclear Magnetic Resonance (NMR) is the phenomenon that certain nuclei behave like tiny spinning bar magnets. In a uniform magnetic field, a proton may take up one of two orientations, which are low-energy and high-energy orientation,

with respect to the field. The transition between these two energy states can be brought by the absorption of a quantum of suitable electromagnetic radiation of energy. In the certain strength of field, the energy required to flip over from one orientation to another can be observed as the nuclear magnetic resonance signal (68). The signals from each proton differ due to the shielding by the electrons surrounding it. This phenomenon is called chemical shift, which corresponds to the structure of the tested molecule. The number of peaks of signal is correspondence to the number of protons attached to adjacent carbon atoms, which called spin-spin coupling. The doublet peak (d) is the signal from the proton attached to the carbon which adjacent to the carbon has one proton. The triplet (t) has the adjacent carbon has two protons. The doublet-doublet (dd) has two adjacent carbons have one proton each. The multiplet (m) has several adjacent carbons, such as aromatic structure (Arom). The singlet (s) has an adjacent carbon does not have a proton. The separation of the peaks in the triplet gives the coupling constant (J). Thus, the chemical shift and coupling constant from the NMR spectrum provide important information to identify the molecular structure, which could be used to ensure the synthesized chemical was the desired product.

The NMR data of synthesized NPPB is shown in Table 3.1:

δ_{H} (500MHz, CDCl_3) 8.77(1H, d, $J=2.4\text{Hz}$, $\text{NO}_2\text{C}-\underline{\text{CH}}=\text{CCO}_2$) 8.46(1H, s, $\underline{\text{NH}}$) 8.15(1H, dd, $J=2.95/9.8\text{Hz}$, $\text{NO}_2\text{C}=\underline{\text{CH}}-\text{CH}$) 7.14~7.28(5H, m, Arom H) 6.73(1H, d, $J=9.8\text{Hz}$, $\underline{\text{CH}}=\text{C}-\text{NH}$) 3.31(2H, m, $\underline{\text{CH}}_2\text{NH}$) 2.74(2H, t, $J=7.7\text{Hz}$, $\underline{\text{CH}}_2-\text{Ph}$) 2.00(2H, m, $\underline{\text{CH}}_2-\text{CH}_2-\text{Ph}$). The data shows the correct number of protons for NPPB and identical to the ^1H NMR result of NPPB from Sigma Chemicals. The final weight of synthesized NPPB was 878mg, producing a 53.26% yield.



Atom Number	Number of protons	$^1\text{H}\delta(\text{ppm})$
1 $\text{NO}_2\text{C}-\underline{\text{CH}}=\text{CCO}_2$	1H	8.77(d, $J=2.4\text{Hz}$)
2 $\text{NO}_2\text{C}=\underline{\text{CH}}-\text{CH}$	1H	8.15(dd, $J=2.95/9.8\text{Hz}$)
3 $\underline{\text{CH}}=\text{C}-\text{NH}$	1H	6.73(d, $J=9.8\text{Hz}$)
4 NH	1H	8.46(s)
5 $\underline{\text{CH}}_2\text{NH}$	2H	3.31(m)
6 $\underline{\text{CH}}_2-\text{CH}_2-\text{Ph}$	2H	2.00(m)
7 $\underline{\text{CH}}_2-\text{Ph}$	2H	2.74(t, $J=7.7\text{Hz}$)
8 Arom H	5H	7.14-7.28(m)

Table 3.1 NMR data of NPPB

3.1.2 PPAB

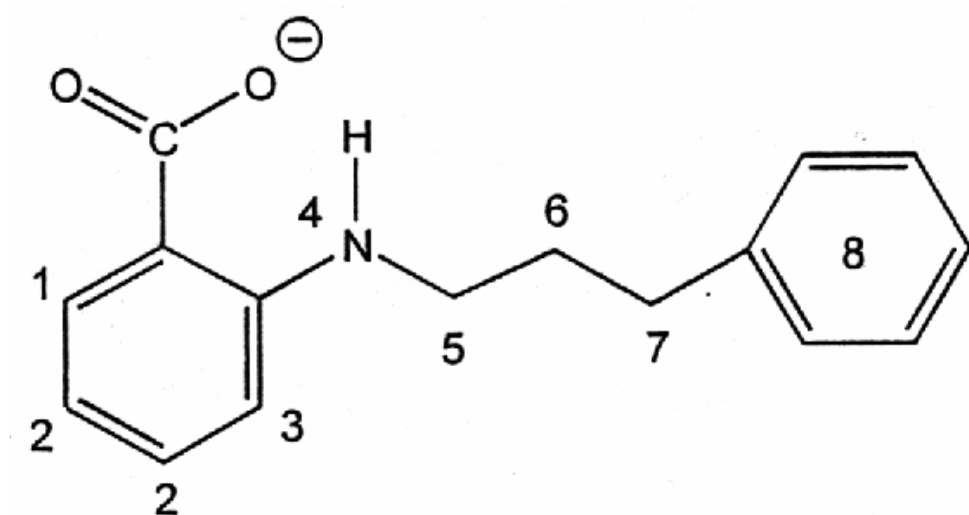
The crude product after the extraction was a slightly brownish white coloured compound. During the extraction, the product tended to remain in the aqueous filtrate. This could be indicated by the purple/pinkish colour of the solution. To achieve a higher yield, the aqueous filtrate had to be back washed by the ethyl acetate and HCl, until the purple/pinkish colour disappears. The final product after the purification was almost white crystals. Almost all impurities were removed by the column chromatography, which was assessed by the TLC. However, some impurities were observed by the ^1H NMR. Therefore the re-crystallization was required to yield pure product.

The NMR data of synthesized PPAB is shown in Table 3.2:

δ_{H} (500MHz, CDCl_3) 7.80~7.98(1H, m, C- $\underline{\text{C}}\text{H}=\text{CCO}_2$)(1H, NH) 7.20~7.40(5H, m, Arom H)(2H, m, $\underline{\text{C}}\text{H}=\underline{\text{C}}\text{H}-\text{CH}=\text{C}-\text{NH}$) 6.61~6.68(1H, m, $\underline{\text{C}}\text{H}=\text{C}-\text{NH}$) 3.24(2H, t, $J=7.14\text{Hz}$, $\underline{\text{C}}\text{H}_2\text{NH}$) 2.77(2H, t, $J=7.53\text{Hz}$, $\underline{\text{C}}\text{H}_2-\text{Ph}$) 2.01~2.07(2H, m, $\underline{\text{C}}\text{H}_2-\text{CH}_2-\text{Ph}$). The data shows the correct number of protons for PPAB and relative to the previous experiment. The final weight of synthesized PPAB was 1.0058g, producing a 54.04% yield.

3.1.3 HANB

The crude product after extraction was a dark yellow coloured compound. Almost all impurities could be removed by the column chromatography. The TLC result suggested the product had no impurities, but in contrast the ^1H NMR result showed the presence of some impurities. The re-crystallization was still required to yield pure product. The final product after the re-crystallization was dark yellow crystals, which was assessed by ^1H NMR in an attempt to show that the crystals were pure HANB.



Atom Number	Number of protons	$^1\text{H}\delta(\text{ppm})$
1 and 4	C- <u>CH</u> =CCO ₂	1H
	N <u>H</u>	1H
2 and 8	<u>CH</u> = <u>CH</u> -CH=C-NH	2H
	Arom H	5H
3	<u>CH</u> =C-NH	1H
5	<u>CH</u> ₂ NH	2H
6	<u>CH</u> ₂ -CH ₂ -Ph	2H
7	<u>CH</u> ₂ -Ph	2H

Table 3.2 NMR data of PPAB

The NMR data of synthesized HANB is shown in Table 3.3:

δ_{H} (500MHz, CDCl_3) 8.94(1H, d, $J=2.78\text{Hz}$, $\text{C}-\underline{\text{C}}\text{H}=\text{CCO}_2$) 8.41(1H, s, NH) 8.24(1H, dd, $J=2.38/9.52\text{Hz}$, $\underline{\text{C}}\text{H}-\text{CH}=\text{C}-\text{NH}$) 6.71(1H, d, $J=9.52$, $\underline{\text{C}}\text{H}=\text{C}-\text{NH}$) 3.30~3.33(2H, m, $\text{HN}-\underline{\text{C}}\text{H}_2$) 1.71~1.77(2H, m, $\text{HN}-\text{CH}_2-\underline{\text{C}}\text{H}_2$) 1.31~1.47(8H, m, $\text{HN}-\text{CH}_2-\text{CH}_2-(\underline{\text{C}}\text{H}_2)^4-\text{CH}_3$) 0.91(3H, t, $J=5.95\text{Hz}$, $\text{CH}_2-\underline{\text{C}}\text{H}_3$). The data shows the correct number of protons for HANB and relative to the previous experiment. The final weight of synthesized HANB was 827mg, producing a 53.72% yield.

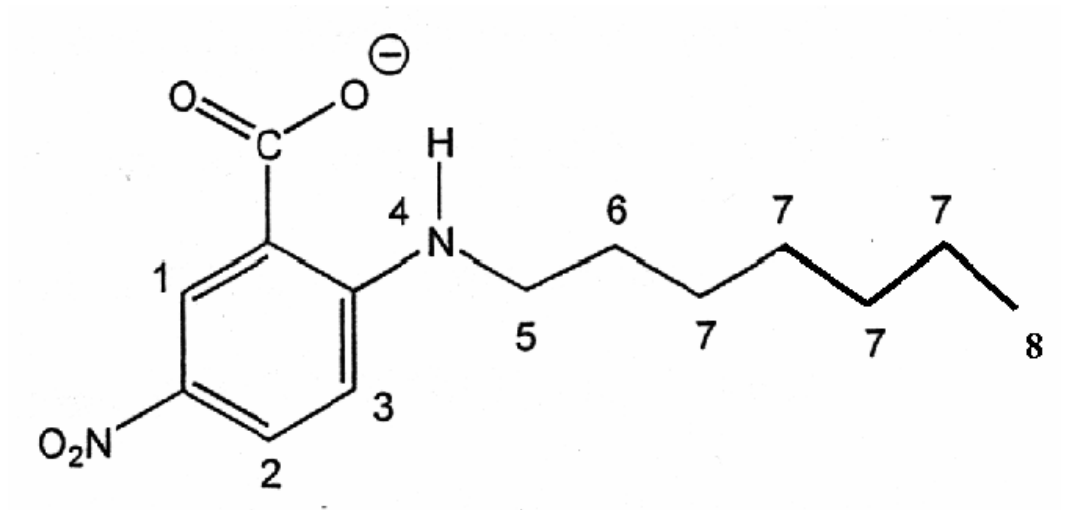
3.1.4 HANB-2

This is the first synthesis of HANB-2. The same procedure was used as NPPB and other analogues. The crude product after extraction was a brown coloured oily type residue. It did not form crystals, so re-crystallization could not be used to purify this product. The column chromatography and the radical silica chromatography performed on chromatatron were used to remove impurities. However, the chromatography had to be run several times to remove impurities. This product was hard to purify.

During the purification process, the purity of the product was assessed by the TLC and ^1H NMR. The final product was assessed by TLC, ^1H NMR, ^{13}C NMR, MS, and IR.

The NMR and IR data of synthesized HANB-2 is shown in Table 3.4:

δ_{H} (500MHz, CDCl_3) 8.00(1H, d, $J=9.12\text{Hz}$, $\text{C}=\underline{\text{C}}\text{H}-\text{CCO}_2$) 7.26(1H, s, NH) 6.65(1H, d, $J=2.38$, $\underline{\text{C}}\text{H}=\text{CH}-\text{C}-\text{NH}$) 6.58~6.60(1H, dd, $J=2.38/9.12$, $\underline{\text{C}}\text{H}-\text{C}-\text{NH}$) 3.21~3.24(2H, t, $J=7.14\text{Hz}$, $\text{HN}-\underline{\text{C}}\text{H}_2$) 1.64~1.70(2H, m, $\text{HN}-\text{CH}_2-\underline{\text{C}}\text{H}_2$) 1.25~1.43(8H, m, $\text{HN}-\text{CH}_2-\text{CH}_2-(\underline{\text{C}}\text{H}_2)^4-\text{CH}_3$) 0.88~0.91(3H, t, $J=6.74\text{Hz}$, $\text{CH}_2-\underline{\text{C}}\text{H}_3$).



Atom Number	Number of protons	$^1\text{H}\delta(\text{ppm})$
1 $\text{NO}_2\text{C}-\underline{\text{CH}}=\text{CCO}_2$	1H	8.94(d, J=2.78Hz)
2 $\underline{\text{CH}}-\text{CH}=\text{C}-\text{NH}$	1H	8.24(dd, J=2.38/9.52Hz)
3 $\underline{\text{CH}}=\text{C}-\text{NH}$	1H	6.71(d, J=9.52)
4 $\underline{\text{NH}}$	1H	8.41(s)
5 $\underline{\text{CH}_2}\text{NH}$	2H	3.30-3.33(m)
6 $\text{HN}-\text{CH}_2-\underline{\text{CH}_2}$	2H	1.71-1.77(m)
7 $\text{HN}-\text{CH}_2-\text{CH}_2-(\underline{\text{CH}_2})^4-\text{CH}_3$	8H	1.31-1.47(m)
8 $\text{CH}_2-\underline{\text{CH}_3}$	3H	0.91(t, J=5.95Hz)

Table 3.3 NMR data of HANB

δ_c (75MHz, CDCl₃) 172.11(COO) 171.72(C-COO) 152.76(C-NH) 134.53(C-NO₂) 131.70(CH=CH-C-NH) 127.42(C=CH-CCO₂) 111.75(CH=CH-C-NH) 43.44(HN-CH₂) 31.66, 28.89, 28.86, 26.84, 22.53(HN-CH₂-(CH₂)⁵-CH₃) 14.11(CH₂-CH₃)

IR (cm⁻¹) 3377.1(-NH) 2927.7(-CH₂-(CH₂)⁵-CH₃) 1714.6(C=O) 1604.7(Arom) 1589.2, 1315.4(-NO₂) 1259.4(C-O).

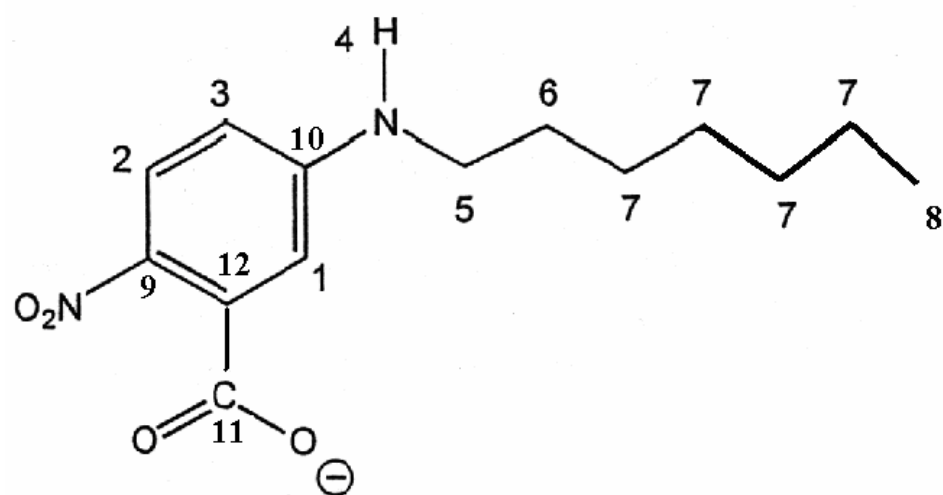
MS also gave the expected parent ion at 281.2 daltons, corresponding to a molecular formula of HANB-2 (C₄H₂₀N₂O₄, 280.32g/mol).

The final product was brown coloured high viscous compound, and the final weight of synthesized HANB-2 was 2.08g, producing a 67.58% yield.

3.2 Cytoplasmic Streaming

The effect of NPPB on cytoplasmic streaming rate is shown in Table 3.5 and 3.6. The data was fitted to a sigmoidal dose-response curve which is shown in Fig3.1 and 3.2. The effect of niflumic acid on streaming rate is shown in Table 3.7 and the corresponding graph is shown in Fig3.3

Because NPPB was not soluble in water, the NPPB solutions were prepared using pH 8 and pH 10 APW. Control experiments were carried out that measured the streaming rate in pH8 and pH10 APW. According to statistical analysis, using a t-test carried out using SigmaPlot (8.02), there was no significant difference between the streaming rates in pH 8 and pH 10 APW. The mean values \pm standard deviation (SD) were 38.37 μ m/s \pm 14.62 and 45.30 μ m/s \pm 8.70 respectively, and they showed P>0.05 in the t-test.



(a)

Atom Number	Number of protons	$^1\text{H}\delta$ (ppm)
1 C=CH-CCO ₂	1H	8.00(d, J=9.12Hz)
2 CH-CH=C-NH	1H	6.65(d, J=2.38Hz)
3 CH=C-NH	1H	6.58-6.60(dd, J=2.38/9.12Hz)
4 NH	1H	7.26(s)
5 CH ₂ NH	2H	3.21-3.24(t, J=7.14Hz)
6 HN-CH ₂ -CH ₂	2H	1.64-1.70(m)
7 HN-CH ₂ -CH ₂ -(CH ₂) ⁴ -CH ₃	8H	1.25-1.43(m)
8 CH ₂ -CH ₃	3H	0.88-0.91(t, J=6.74Hz)

(b)

Atom Number	$^{13}\text{C}\delta(\text{ppm})$	
1	$\text{C}=\underline{\text{C}}\text{H}-\text{CCO}_2$	127.42
2	$\underline{\text{C}}\text{H}-\text{CH}=\text{C}-\text{NH}$	131.7
3	$\text{CH}-\underline{\text{C}}\text{H}=\text{C}-\text{NH}$	111.75
5	$\text{HN}-\underline{\text{C}}\text{H}_2$	43.44
6 and 7	$\text{HN}-\text{CH}_2-(\underline{\text{C}}\text{H}_2)^5-\text{CH}_3$	31.66, 28.89, 28.86, 26.84, 22.53
8	$\text{CH}_2-\underline{\text{C}}\text{H}_3$	14.11
9	$\underline{\text{C}}-\text{NO}_2$	134.53
10	$\underline{\text{C}}-\text{NH}$	152.76
11	$\underline{\text{C}}\text{OOH}$	172.11
12	$\underline{\text{C}}-\text{COOH}$	171.72

(c)

Functional Group	IR (cm^{-1})
NH	3377.1
$\text{CH}_2-(\text{CH}_2)^5-\text{CH}_3$	2927.7
C=O	1714.6
Arom	1604.7
NO_2	1315.4, 1589.2
C-O	1259.4

Table 3.4 NMR and IR data of HANB-2

(a) ^1H NMR

(b) ^{13}C NMR

(c) IR.

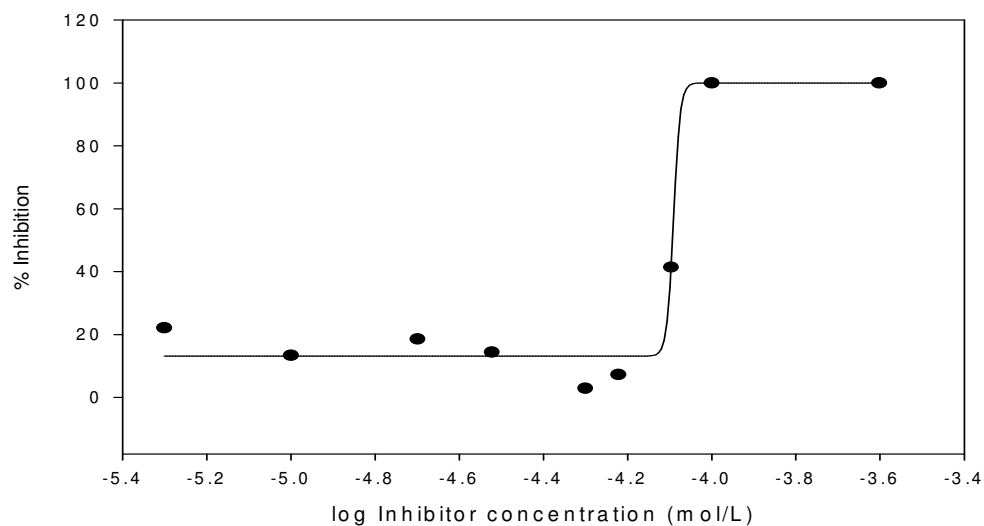
The data, when fitted to a sigmoidal dose-response curve, was used to calculate IC_{50} values for each inhibitor solution. The IC_{50} value (expressed as concentration of inhibitor) is the concentration of inhibitor which inhibits streaming to 50% of the maximal rate. The lower the value means the more potent the inhibitor.

The data for NPPB in pH 8 APW is shown in Table 3.5 and has been fitted to a sigmoidal dose-response curve which is shown in Fig3.1. According to the sigmoidal dose-response curve, an IC_{50} value of $81.28\mu\text{mol/L}$ after 5 minutes exposure to the inhibitor solution, and $80.00\mu\text{mol/L}$ after 10 minutes exposure. The data for NPPB in pH 10 APW is shown in Table 3.6 and the sigmoidal dose-response curve is shown in Fig3.2. The sigmoidal dose-response curve gave an IC_{50} value of $100\mu\text{mol/L}$ after 5 minutes exposure to the inhibitor solution, and $93.33\mu\text{mol/L}$ after 10 minutes exposure.

Both NPPB solutions showed slightly lower IC_{50} values after 10 minutes exposure compared to 5 minutes exposure, which means longer contact with the inhibitor may affect the streaming rate. However, the difference of IC_{50} values between 5 minutes and 10 minutes exposure were too subtle to actually be significantly difference.

The recovery of cytoplasmic streaming rate in the absence of the inhibitor was measured at 10 and 20 minutes after the cells were reimmersed in APW. A statistical analysis (t-test) was performed comparing streaming rates in $80\mu\text{mol/L}$ of NPPB in pH 8 and $50\mu\text{mol/L}$ of NPPB in pH 10. The rates at both 10 and 20 minutes after reimmersion in APW from pH 8 NPPB solution were $31.42\mu\text{m/s} \pm 8.59$ and $30.68\mu\text{m/s} \pm 7.63$ respectively. The t-test analysis showed the significant differences as $P < 0.05$, which effectively means that the

(a)



(b)

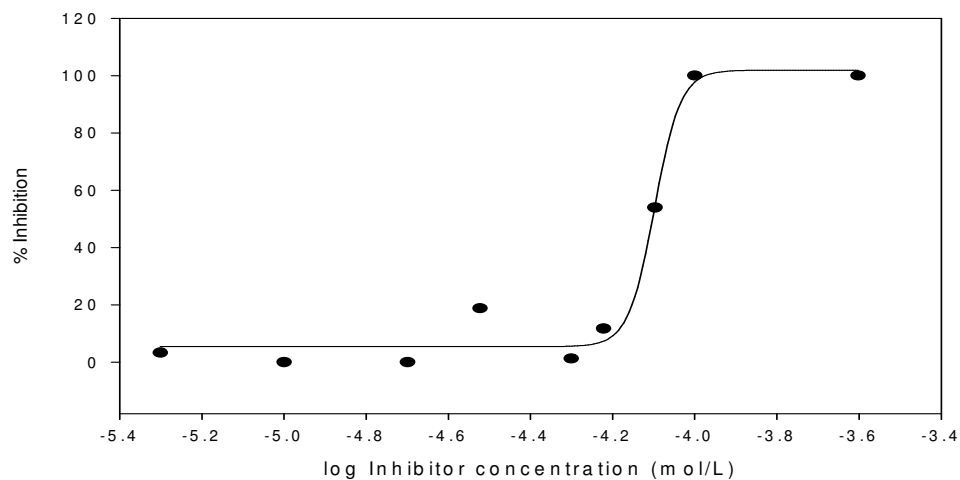


Figure 3.1 Dose-response curve for NPPB in pH 8 APW.

(a) cells exposed to the inhibitor solution for 5 minutes.

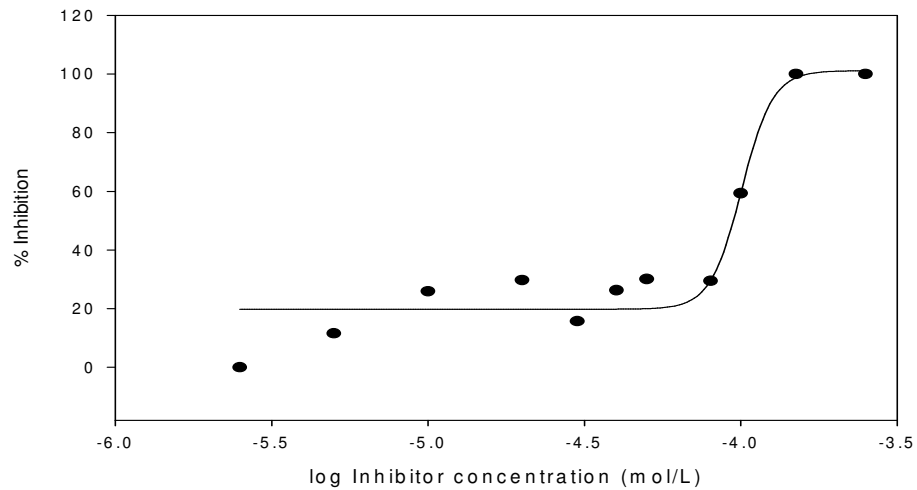
(b) cells exposed to the inhibitor solution for 10 minutes.

The % inhibition was calculated as the streaming rate reduction of the cells immersed in NPPB (pH 8) solution, compared to the streaming rate of the cells in APW. Data have been fitted to a dose-response curve of the form $y = \min + ((\max - \min) / (1 + 10^{\log IC_{50} - x \cdot \text{hill slope}}))$ calculated using the ligand-binding module of SigmaPlot (8.02).

Concentration			Streaming Rate ($\mu\text{m/s}$) and % inhibition				
(μM)	(mol/L)	LOG ¹⁰	APW	Inh-5min	% Inh-5min	Inh-10min	% Inh-10min
5	0.000005	-5.30	34.04	26.51	22.12	32.91	3.32
10	0.00001	-5.00	27.45	23.78	13.37	31.86	0.00
20	0.00002	-4.70	28.70	23.38	18.54	37.14	0.00
30	0.00003	-4.52	55.56	47.56	14.40	45.09	18.84
50	0.00005	-4.30	18.97	18.42	2.90	18.72	1.32
60	0.00006	-4.22	54.25	50.32	7.24	47.89	11.72
80	0.00008	-4.10	49.60	29.06	41.41	22.84	53.95
100	0.00010	-4.00			100.00		100.00
250	0.00025	-3.60			100.00		100.00
				IC ₅₀	-4.09		-4.10
					81.28 μM		80.00 μM

Table 3.5 The effect of NPPB (pH 8) on cytoplasmic streaming rate. Inh-5min and Inh-10min are the streaming rates of the cells which were immersed in pH 8 NPPB solution for 5 minutes and 10 minutes, respectively. 100% inhibition signifies the complete cessation of streaming. IC₅₀ value was determined from dose-response curve (Fig. 3.1).

(a)



(b)

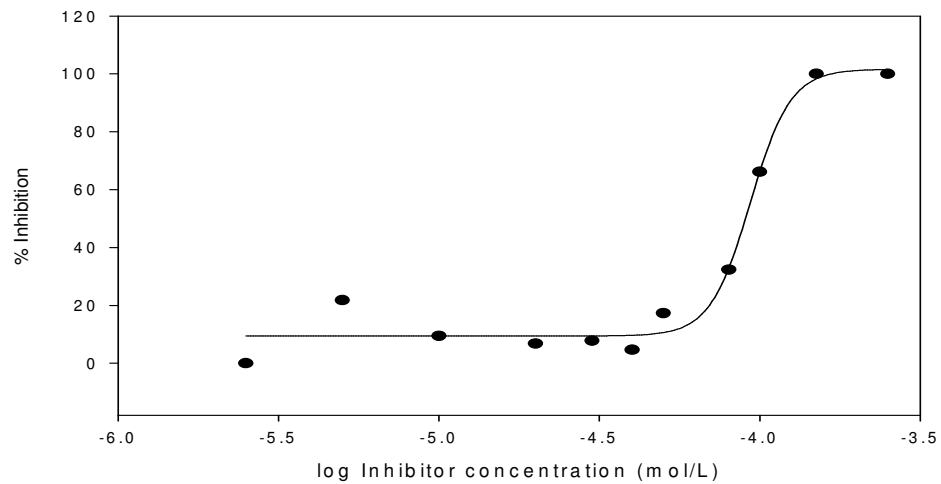


Figure 3.2 Dose-response curve for NPPB in pH 10 APW.

(a) cells exposed to the inhibitor solution for 5 minutes.

(b) cells exposed to the inhibitor solution for 10 minutes.

The % inhibition was calculated as the streaming rate reduction of the cells immersed in NPPB (pH 10) solution, compared to the streaming rate of the cells in APW. Data have been fitted to a dose-response curve of the form $y = \text{min} + ((\text{max} - \text{min}) / (1 + 10^{\log \text{IC}_{50} - x \cdot \text{hillslope}}))$ calculated using the ligand-binding module of SigmaPlot (8.02).

Concentration			Streaming Rate ($\mu\text{m/s}$) and % inhibition				
(μM)	(mol/L)	LOG ¹⁰	APW	Inh-5min	% Inh-5min	Inh-10min	% Inh-10min
2.5	0.0000025	-5.60	40.14	45.09	0.00	51.44	0.00
5	0.000005	-5.30	37.95	33.55	11.59	29.68	21.79
10	0.00001	-5.00	48.56	35.98	25.91	43.95	9.49
20	0.00002	-4.70	56.46	39.68	29.72	52.61	6.82
30	0.00003	-4.52	58.85	49.60	15.72	54.25	7.82
40	0.00004	-4.40	48.56	35.80	26.28	46.30	4.65
50	0.00005	-4.30	36.36	25.44	30.03	30.06	17.33
80	0.00008	-4.10	34.55	24.37	29.46	23.38	32.33
100	0.00010	-4.00	46.30		*59.32		*66.17
150	0.00015	-3.82			100.00		100.00
250	0.00025	-3.60			100.00		100.00
				IC ₅₀	-4.00		-4.03
					100 μM		93.33 μM

Table 3.6 The effect of NPPB (pH 10) on cytoplasmic streaming rate. Inh-5min and Inh-10min are the streaming rates of the cells which were immersed in pH 10 NPPB solution for 5 minutes and 10 minutes, respectively. 100% inhibition signifies the complete cessation of streaming. IC₅₀ value was determined from dose-response curve (Fig. 3.2).

*Some of samples showed complete cessation of streaming. The % inhibition was calculated by taking the average of % inhibition of each sample with stating the complete cessation as 100%

effect of NPPB in pH 8 APW is irreversible. On the other hand, there is no significant difference between the initial cytoplasmic streaming rate and the rate at 10 and 20 minutes after reimmersion in APW from pH 10 NPPB solution, which were $40.66\mu\text{m/s} \pm 13.52$ and $41.66\mu\text{m/s} \pm 13.79$ respectively as $P > 0.05$, which essentially means that the inhibition effect of NPPB in pH 10 APW is reversible.

The data for niflumic acid in pH 8 APW is shown in Table 3.7 and was fitted to the sigmoidal dose-response curve as shown in Fig3.3. According to the sigmoidal dose-response curve, it gave an IC_{50} value of $128.82\mu\text{mol/L}$ after 5 minutes exposure to the inhibitor solution, and $114.82\mu\text{mol/L}$ after 10 minutes exposure. A statistical analysis (t-test) was performed on streaming rates at these exposure times to $50\mu\text{mol/L}$ of niflumic acid. The rate after 10 minutes after reimmersion in APW was significantly different to the initial cytoplasmic streaming rate ($P < 0.05$), while the rate after 20 minutes showed no difference ($P > 0.05$). The data may suggest that the inhibitory effect of niflumic acid on cytoplasmic streaming is reversible, but it takes more than 10 minutes to recover.

3.3 Turgor Regulation

Firstly, the turgor pressure of internodal cells of *Nitella hookeri* in APW was measured. The pH of APW was adjusted pH to 8. The average turgor pressure \pm standard deviation (SD) of cells in APW was $7.44\text{MPa} \pm 0.99$ ($n=18$).

As for the turgor regulation experiment with hyperosmotic solution, APW containing D-sorbitol was used as hyperosmotic solution. In hyperosmotic solution, water tends to flow out from inside to the outside of cells through the

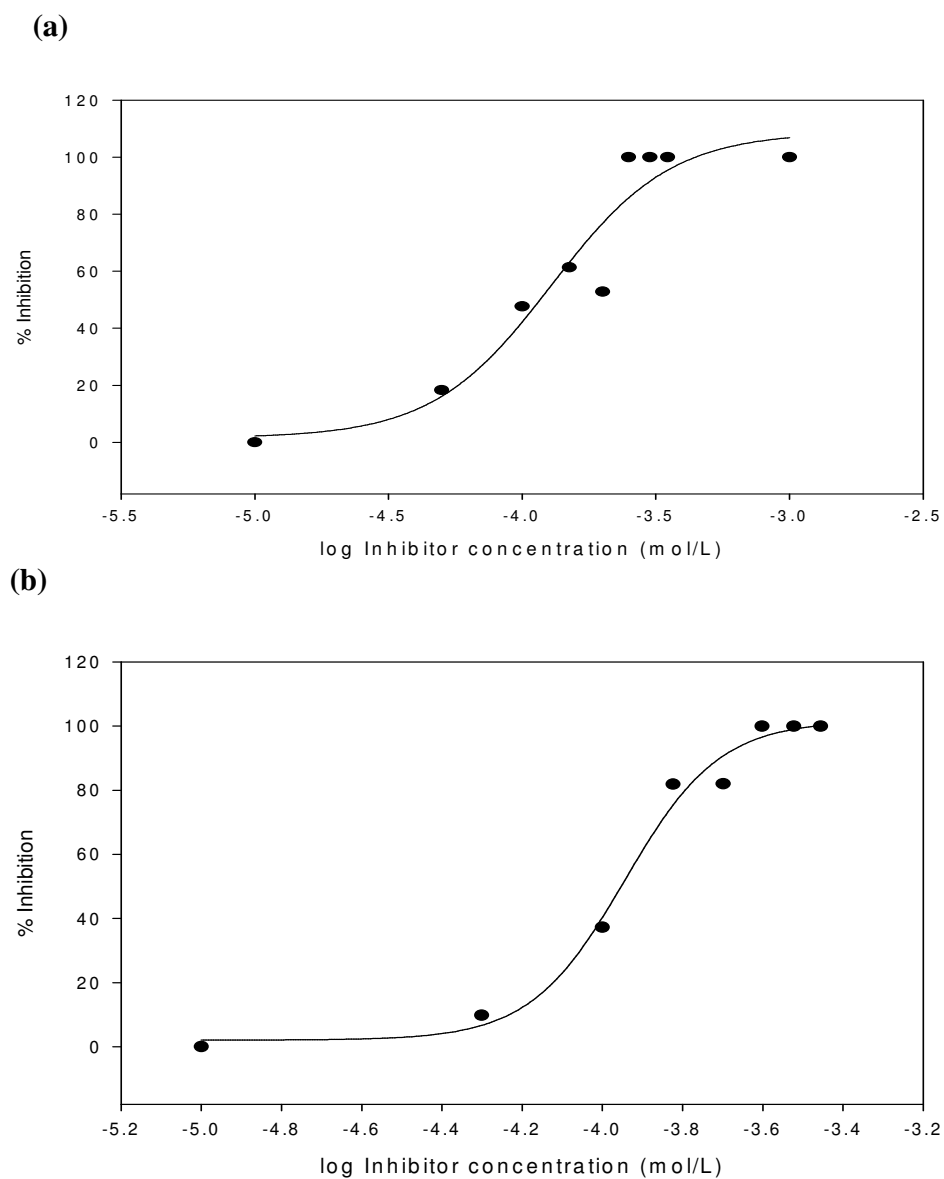


Figure 3.3 Dose-response curve for Niflumic acid in pH 8 APW.

(a) cells exposed to the inhibitor solution for 5 minutes.

(b) cells exposed to the inhibitor solution for 10 minutes.

The % inhibition was calculated as the streaming rate reduction of the cells immersed in Niflumic acid solution, comparing to the streaming rate of the cells in APW. Data have been fitted to a dose-response curve of the form $y = \text{min} + ((\text{max} - \text{min}) / (1 + 10^{\log \text{IC}_{50-x} \text{ hillslope}}))$ calculated using the ligand-binding module of SigmaPlot (8.02).

Concentration			Streaming Rate ($\mu\text{m/s}$) and % inhibition				
(μM)	(mol/L)	LOG ¹⁰	APW	Inh-5min	% Inh-5min	Inh-10min	% Inh-10min
10	0.00001	-5.00	48.90	49.25	0.00	54.25	0.00
50	0.00005	-4.30	44.52	36.36	18.33	40.14	9.84
100	0.00010	-4.00	39.91	20.88	47.68	25.05	37.23
150	0.00015	-3.82	52.61	20.33	61.36	9.55	81.85
200	0.00020	-3.70	58.85	27.75	52.85	10.56	82.06
250	0.00025	-3.60	48.56		100.00		100.00
300	0.00030	-3.52	36.36		100.00		100.00
350	0.00035	-3.46			100.00		100.00
1000	0.00100	-3.00			100.00		100.00
				IC ₅₀	-3.89		-3.94
					128.82 μM		114.82 μM

Table 3.7 The effect of Niflumic acid (pH 8) on cytoplasmic streaming rate. Inh-5min and Inh-10min are the streaming rate of the cells which were immersed in Niflumic acid solution for 5 minutes and 10 minutes, respectively. 100% inhibition signifies the complete cessation of streaming. IC₅₀ value was determined from dose-response curve (Fig. 3.3).

cell membrane. Therefore, the sample cells in higher concentrations of hyperosmotic solution lost rigidity, which made it difficult to impale the microcapillary into the cells in order to measure turgor pressure using the pressure probe. Several different concentrations of hyperosmotic solution were tested for the pressure probe measurement to identify the most workable concentration, which was taken as the highest concentration that enabled pressure probe impalement and at the same time showed sufficient turgor change. In this research, the APW containing 100mM of sorbitol was used as the hyperosmotic solution, in which cells had a mean turgor pressure \pm SD of $5.08\text{MPa} \pm 0.45$ (n=14). For the inhibitor experiments with PPAB, the hyperosmotic solution, which was adjusted its pH to 10, was used, because of the insolubility of PPAB. The turgor pressure of cells in the pH 10 hyperosmotic solution was $4.82\text{MPa} \pm 0.43$ (n=12). A statistical analysis, using a t-test carried out using SigmaPlot (8.02), showed no significant difference between the turgor pressure in pH 8 and pH 10 hyperosmotic solution giving a $P > 0.05$. Regardless of APW pH the internodal cells in hyperosmotic solutions showed significantly reduced turgor pressure comparing with cells in APW.

The effect of NPPB on turgor pressure in the hyperosmotic solution is shown in Table 3.8. For the inhibitor experiments with NPPB, a hyperosmotic solution containing 100, 50 and $25\mu\text{M}$ of NPPB was used and gave mean turgor pressure \pm SD readings were 6.15 ± 0.87 (n=12), 6.35 ± 0.99 (n=9), and $5.22\text{MPa} \pm 0.48$ (n=11), respectively. The differences in turgor pressure between APW and hyperosmotic solution with/without NPPB are summarized in Fig 3.4 along with the calculated osmotic potential of each solution. The effect of NPPB was to inhibit turgor regulation in the hyperosmotic solution, thus rather than turgor remaining constant there was a significant reduction of turgor pressure. The cells treated in hyperosmotic solution containing $100\mu\text{M}$

and 50 μ M of NPPB showed a slight reduction of turgor pressure compared with APW, but not as much reduction as the pressure in the hyperosmotic solution without NPPB. Also the effect of NPPB was dose dependent. The turgor pressure in the hyperosmotic solution containing 25 μ M NPPB showed no significant difference ($P>0.05$) from that in the hyperosmotic solution without NPPB, while 50 μ M NPPB solution, (6.35MPa) showed significant inhibition of the turgor regulation relative to the hyperosmotic solution without NPPB, (5.08MPa). The 100 μ M NPPB solution also showed the inhibition of the turgor regulation (6.15MPa), but this effect was not as large as that of the 50 μ M NPPB solution. However, a t-test stated no significant different ($P>0.05$) between the measurements of 50 and 100 μ M NPPB. One possible explanation for the larger effect with 50 mM NPPB and the t-test result may have been that above 50mM the NPPB does not readily solubilise and so the effective concentration was somewhat lower than 100 mM.

The effect of PPAB on turgor pressure in the hyperosmotic solution is shown in Table 3.9 For the inhibitor experiments with PPAB, a hyperosmotic solution containing 500, 250 and 50 μ M of PPAB was used, and these gave turgor pressure \pm SD readings were 5.93 \pm 0.71 (n=11), 5.19 \pm 0.39 (n=12), and 5.30MPa \pm 0.63 (n=13), respectively. The turgor pressure in the hyperosmotic solution adjusted pH to 10 was 4.82MPa \pm 0.43 (n=12). The differences in turgor pressure readings between APW and hyperosmotic solution with/without PPAB are summarized in Fig 3.5 along with the osmotic potential of each solution. PPAB showed similar effect as NPPB in that it inhibited turgor regulation in hyperosmotic solution of pH 10. The cells treated in hyperosmotic solution containing PPAB showed a slight reduction of turgor pressure compared with APW, but not as much as a reduction as with the hyperosmotic solution without PPAB. The effect of PPAB also showed dose

Sample solution	Osmolality (mol/kg)	Osmotic potential (MPa)	Turgor Pressure (MPa)
APW	0.044	0.11	7.44
100mM Sorbitol/APW	0.111	0.27	5.08
100μM NPPB in S/A	0.101	0.25	6.15
50μM NPPB in S/A	0.109	0.27	6.35
25μM NPPB in S/A	0.108	0.26	5.22

Table 3.8 The effect of NPPB (pH8) on turgor regulation in hyperosmotic solution (100mM Sorbitol in APW). S/A is used as an abbreviation of this hyperosmotic solution. Osmolality was measured using a vapor pressure osmometer, and osmotic potential was calculated by the equation; $\pi=CRT$ where C=osmolality, R=universal gas constant, and T=absolute temperature.

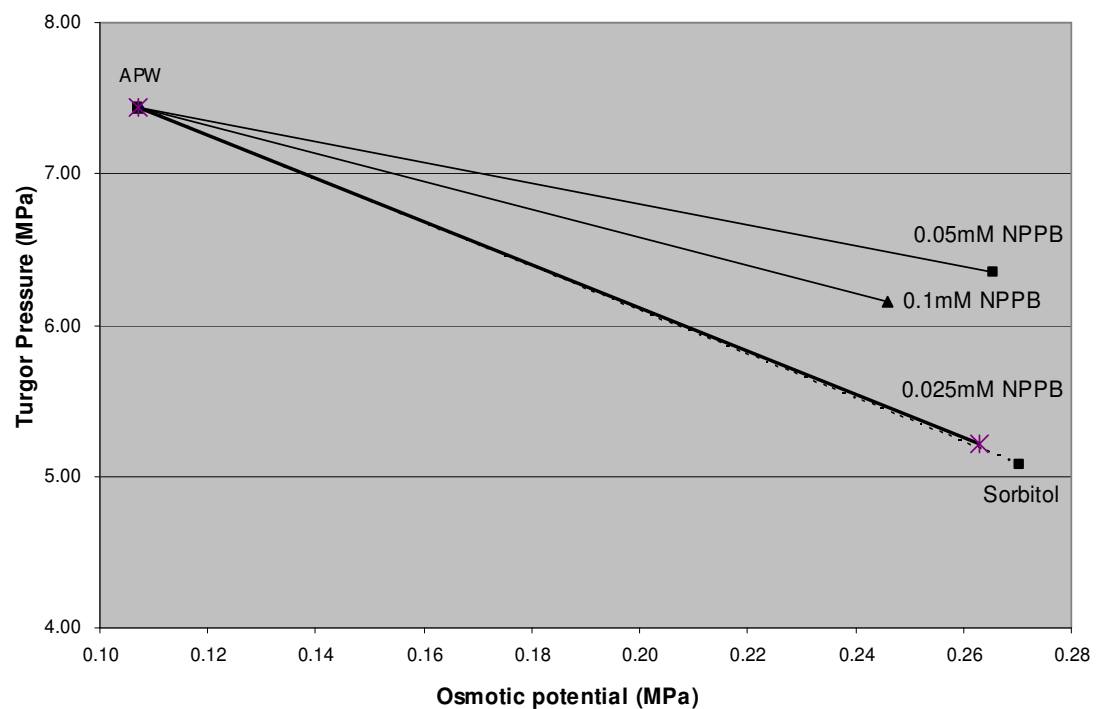


Figure 3.4 The effect of NPPB on turgor regulation in the hyperosmotic solution, comparing with the turgor pressure in APW, (from the data shown in Table 3.8.)

Sample solution	Osmolality (mol/kg)	Osmotic potential (MPa)	Turgor regulation (MPa)
APW	0.044	0.11	7.44
100mM Sorbitol/APW	0.112	0.27	4.82
500 μ M PPAB in S/A	0.102	0.25	5.93
250 μ M PPAB in S/A	0.105	0.26	5.19
50 μ M PPAB in S/A	0.106	0.26	5.30

Table 3.9 The effect of PPAB (pH10) on turgor regulation in hyperosmotic solution (100mM Sorbitol in APW). S/A is used as an abbreviation of this hyperosmotic solution. Osmolality was measured using a vapor pressure osmometer, and osmotic potential was calculated by the equation; $\pi=CRT$ where C=osmolality, R=universal gas constant, and T=absolute temperature.

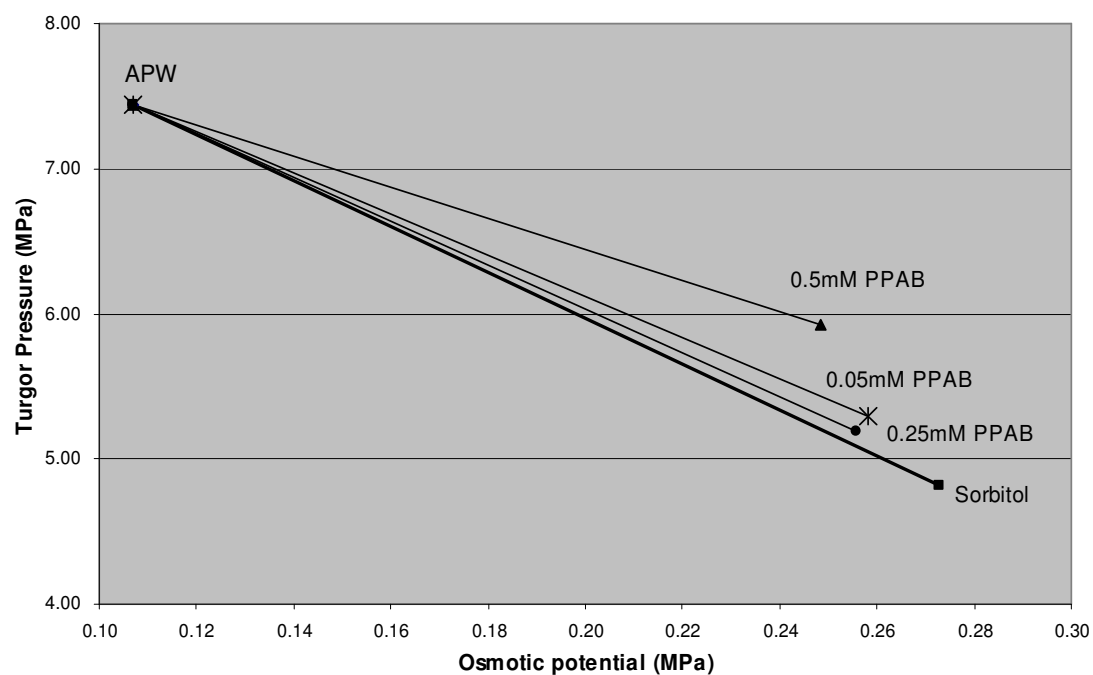


Figure 3.5 The effect of PPAB on turgor regulation in the hyperosmotic solution, comparing with the turgor pressure in APW (from the data shown in Table 3.9)

dependence. The turgor pressure in the hyperosmotic solution containing 50 μ M of PPAB showed higher a reading of turgor pressure than that with 250 μ M PPAB, which contradicts the dose dependent manner of inhibition somewhat. However, again a t-test result suggested that there was no significant difference between these two concentrations ($P>0.05$), also both measurements are significantly different ($P<0.05$) from the turgor pressure measurement of the hyperosmotic solution. Thus, the effect of PPAB on turgor regulation in hyperosmotic solution was also observed as the inhibition of lowering turgor pressure in the hyperosmotic solution.

With regard to the osmotic potential of the hyperosmotic solution with/without inhibitors, the osmotic potential of all concentrations of NPPB and PPAB solution was between 0.25 to 0.27MPa, while the osmotic potential of pH 8 and pH 10 hyperosmotic solution was also 0.27MPa. Thus it can be concluded that there effects of the inhibitor solutions are due to the inhibitor molecules themselves and not due to a change in the osmotic potential of the medium bathing the cells once the inhibitor solution was added.

3.4 Cytosolic Free Calcium Analysis

It has been reported that the treatment of aequorin transformed cells under low temperature (0~5 $^{\circ}$ C) induces Ca²⁺ influx into the cytosol of plant cells (59). Thus cold-shock treated aequorin transformed cells were used as the control for this set of experiments. The cytosolic Ca²⁺ level of control cells was found to suddenly increase around 1 minute and 20 seconds after the measurement started and ceased immediately, the Ca²⁺ level then gradually fell to the normal level by 2 minutes. The average increase of cytosolic free Ca²⁺ of the control was 4.88 μ M (Fig 3.6). The presence of a calcium

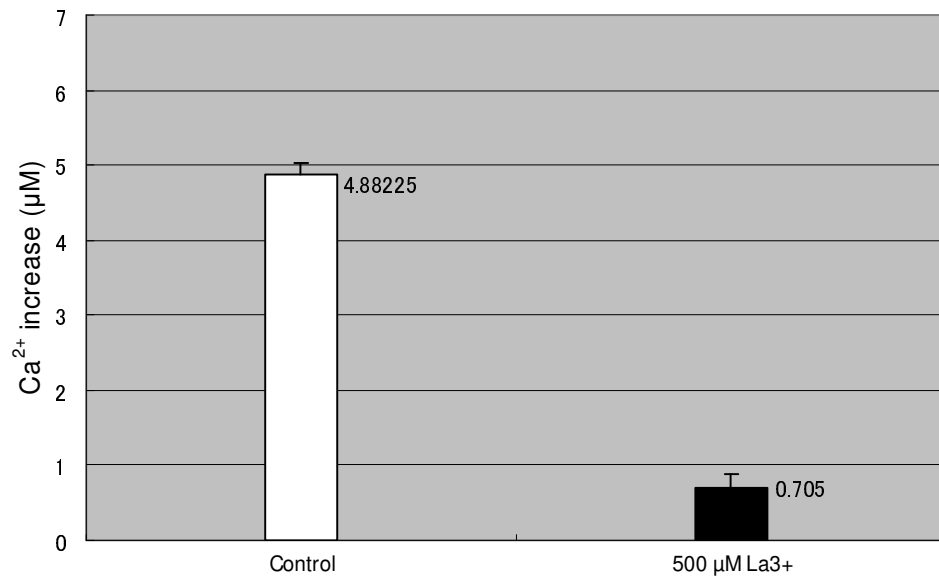


Figure 3.6 The average increase of the concentration of cytosolic free Ca²⁺ in aequorin transformed cells with/without a calcium surrogate (La³⁺). The cold-shock treatment at 0~5°C has been performed to the cells to induce Ca²⁺ influx.

surrogate (La^{3+}) reduced the increase of Ca^{2+} level to $0.7\mu\text{M}$. Thus, any effects of the ion channel inhibitors (NPPB, PPAB, and HANB) could be indicated by comparing the average increase of cytosolic free Ca^{2+} in the cold-shock treated aequorin transformed cells.

3.4.1 NPPB

The effect of 1mM NPPB on the concentration of cytosolic free Ca^{2+} in the cold-shock treated aequorin transformed cells is shown in Fig 3.7a. The change of Ca^{2+} level of the cold shock treated cells with NPPB showed a similar response as the control. The Ca^{2+} level rose at 1 minute and 4 seconds after the measurement started, and then dropped to the normal level within 20 seconds. Thus, the dynamics of Ca^{2+} influx induced by the cold shock was also observed in the cells with NPPB.

However, the average increase of cytosolic free Ca^{2+} was reduced by NPPB in a dose dependent manner, as shown in Fig 3.7b. The average increase of Ca^{2+} level of the control was $4.607\mu\text{M}$. The presence of NPPB reduced this value from $4.607\mu\text{M}$ to $2.452\mu\text{M}$ at a concentration of 1mM and to $2.621\mu\text{M}$ at a concentration of $100\mu\text{M}$, suggesting that NPPB affects plasma membrane Ca^{2+} channels in the aequorin transformed cells.

The average increases in Ca^{2+} level with $75\mu\text{M}$, $50\mu\text{M}$, $25\mu\text{M}$, and $10\mu\text{M}$ of NPPB were $4.907\mu\text{M}$, $4.828\mu\text{M}$, $4.292\mu\text{M}$, and $4.150\mu\text{M}$, respectively. These values were similar to the value of the control, which indicated the dose dependent manner of NPPB and the effective dose of NPPB needed to reduce the Ca^{2+} influx to the cytosol of the plant cells (*Nicotiana plumbaginifolia*) is be greater than $100\mu\text{M}$.

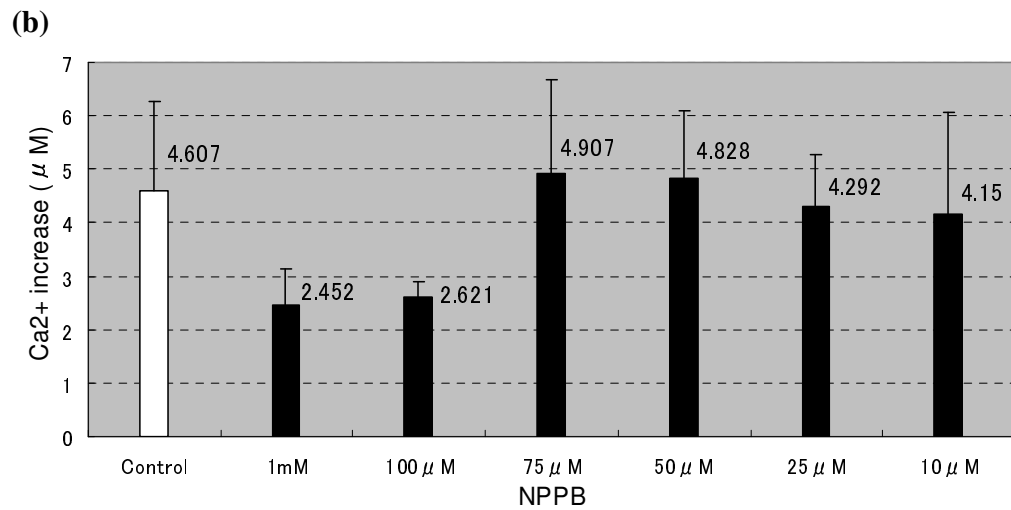
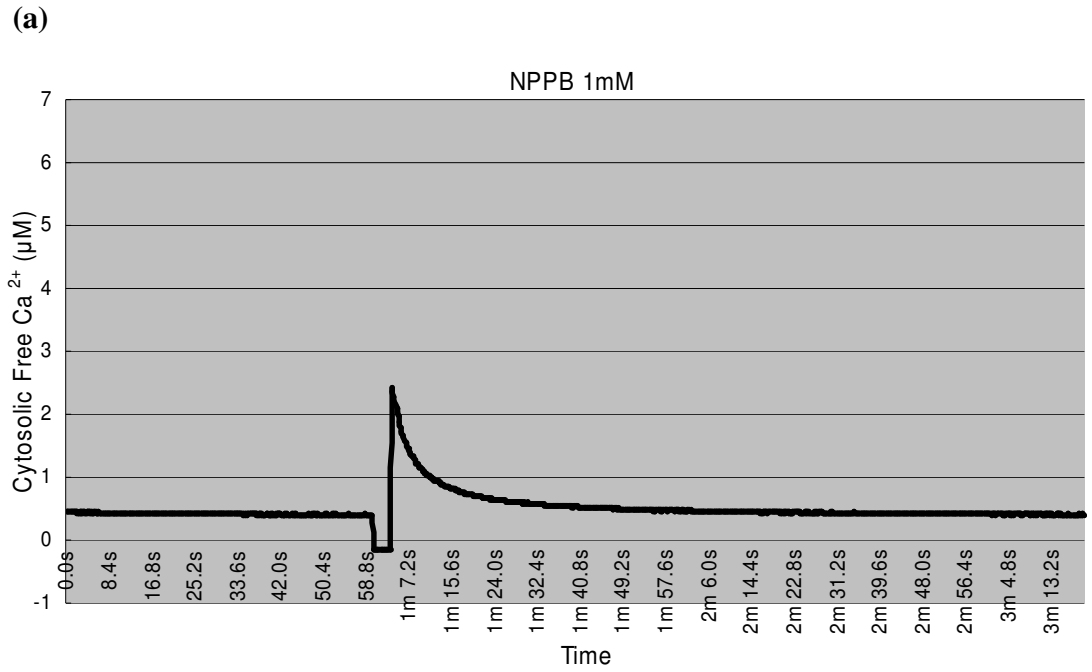


Figure 3.7 The effects of NPPB on the concentration of cytosolic free Ca²⁺ in aequorin transformed cells, which were treated at 0~5°C to induce Ca²⁺ influx. (a) Changes in the concentration of cytosolic free Ca²⁺ in aequorin transformed cells with NPPB (1mM). (b) The total increase of cytosolic free Ca²⁺ with presence of different concentration of NPPB (1mM, 100, 75, 50, 25, 10 μM).

3.4.2 PPAB

The effects of 1mM PPAB on the concentration of cytosolic free Ca^{2+} in the cold-shock treated aequorin transformed cells is shown in Fig 3.8a. As for NPPB, PPAB also showed similar pattern of Ca^{2+} influx with the cold-shock induced cells. The Ca^{2+} influx was observed at 45 seconds after the measurement started, and fell to the normal level at 1 minute and 20 seconds.

The average increase of Ca^{2+} level with PPAB is shown in Fig 3.8b. One mM of PPAB decreased the Ca^{2+} increase level from $4.88\mu\text{M}$ to $0.86\mu\text{M}$, which suggesting the presence of PPAB disrupts the Ca^{2+} influx that is induced by the cold-shock.

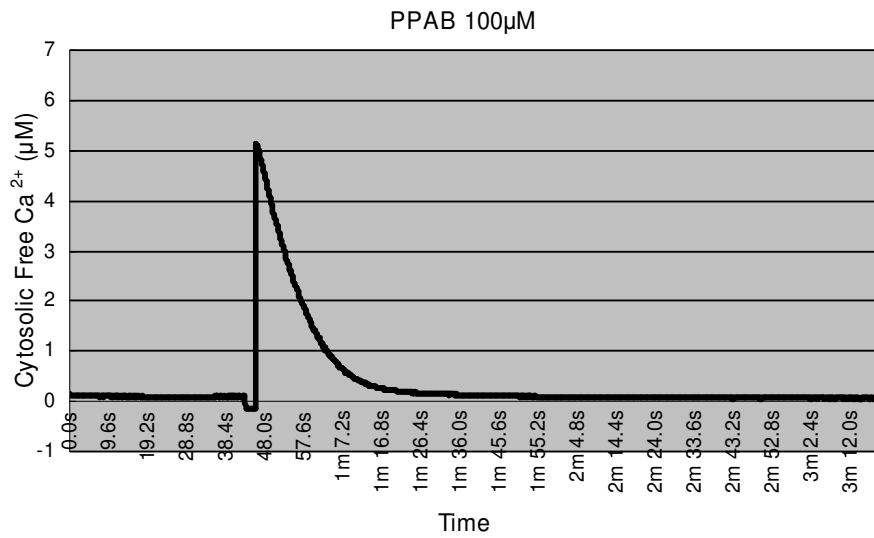
However, while 1mM PPAB showed a significant reduction in the increase of Ca^{2+} level in the cytosol, $100\mu\text{M}$ of PPAB did not show an effect on the Ca^{2+} influx. The average increase of cytosolic free Ca^{2+} with $100\mu\text{M}$ of PPAB was $4.87\mu\text{M}$, which shows no significant difference from the Ca^{2+} increase level of the control. Thus as for NPPB, PPAB also has an effect on the plasma membrane Ca^{2+} channels in with the most effective dose of PPAB between $100\mu\text{M}$ and 1mM.

3.4.3 HANB

The effects of 1mM HANB on the concentration of cytosolic free Ca^{2+} in the cold-shock treated aequorin transformed cells is shown in Fig 3.9a. HANB also showed a similar pattern of Ca^{2+} influx into the cytosol. Moreover, the average increase of cytosolic Ca^{2+} level was also similar to the value of the control, which suggests no effect of HANB on the increase of cytosolic Ca^{2+} . The average increase of Ca^{2+} level with HANB is shown in Fig 3.9b where the value was $4.38\mu\text{M}$, while the control has the value of $4.88\mu\text{M}$.

However, HANB also interfered with the biochemical reaction allowing the luminescence. HANB tended to absorb the blue light, which is released from the aequorin complex upon binding of Ca^{2+} . Because the quantitative analysis of Ca^{2+} in the cytosol using aequorin technology is reliant on the luminescence measurements of the emitted light from the aequorin complex, the ability to absorb the light would affect the accuracy of the results. Therefore, the ineffectiveness of HANB on the plasma membrane Ca^{2+} channel may be caused by the light absorbing ability of the HANB molecules.

(a)



(b)

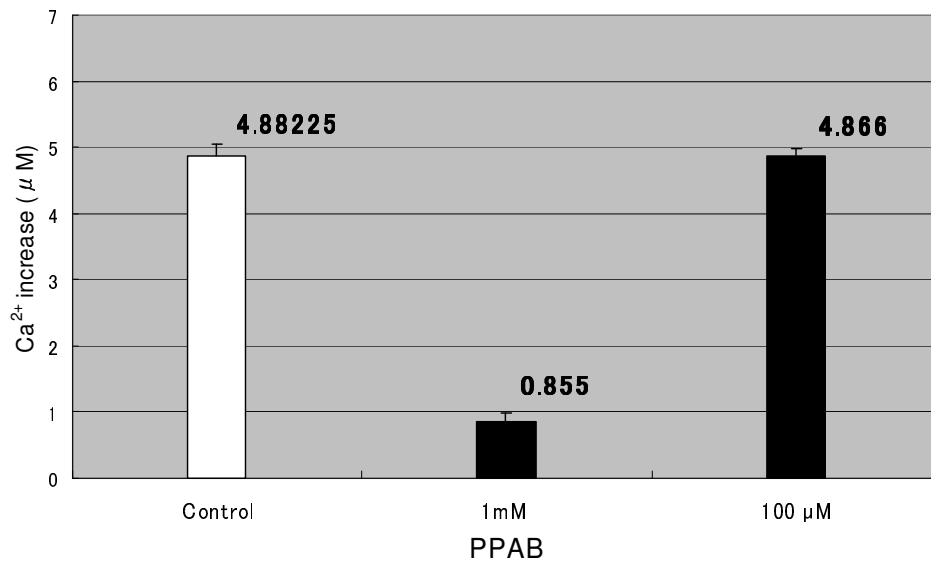


Figure 3.8 The effects of PPAB on the concentration of cytosolic free Ca²⁺ in aequorin transformed cells, which were treated at 0~5°C to induce Ca²⁺ influx. (a) Changes in the concentration of cytosolic free Ca²⁺ in aequorin transformed cells with PPAB (100µM). (b) The total increase of cytosolic free Ca²⁺ with presence of different concentration of PPAB (1mM and 100µM).

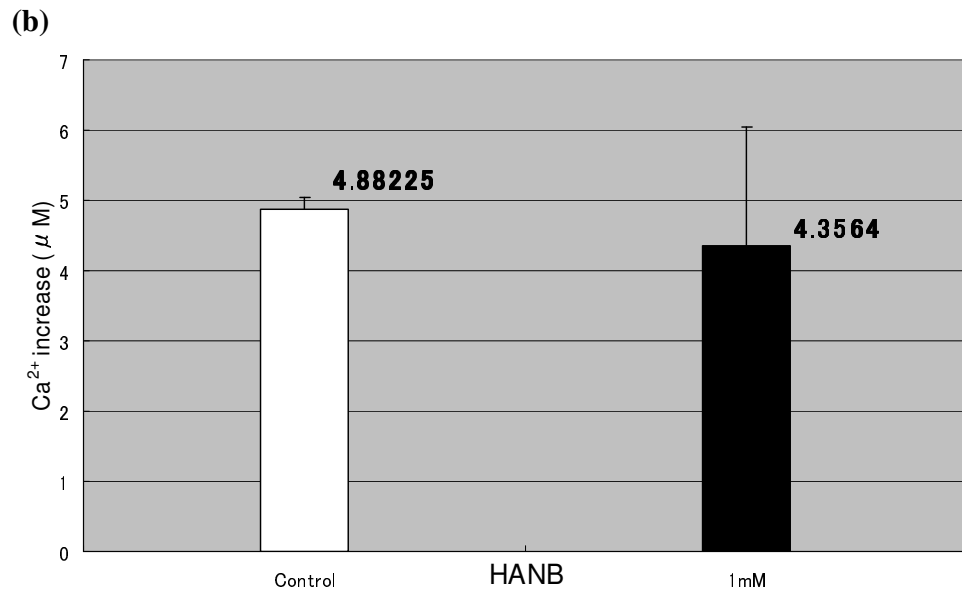
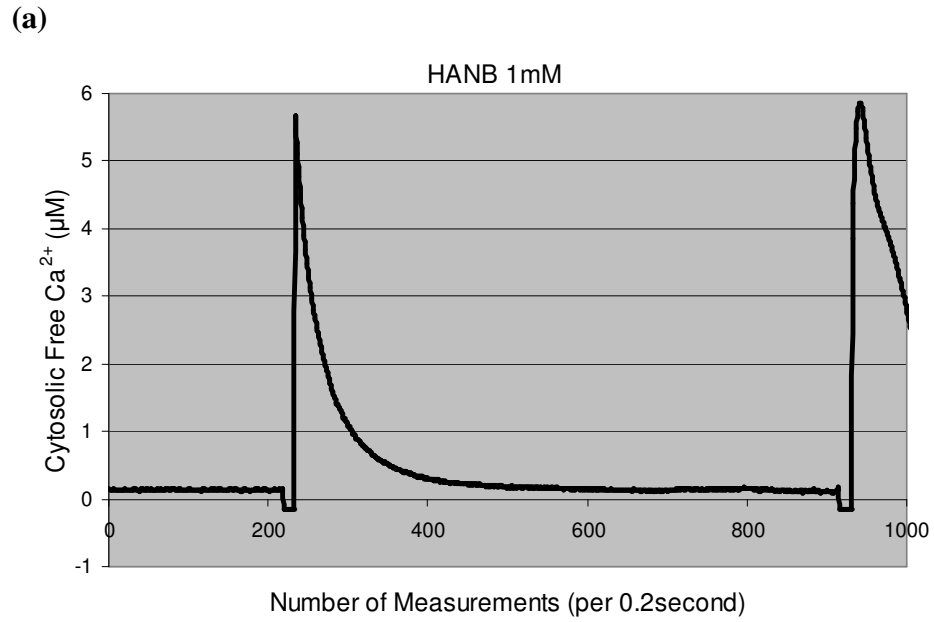


Figure 3.9 The effects of HANB on the concentration of cytosolic free Ca²⁺ in aequorin transformed cells, which were treated at 0~5°C to induce Ca²⁺ influx.
 (a) Changes in the concentration of cytosolic free Ca²⁺ in aequorin transformed cells with HANB (1mM).
 (b) The total increase of cytosolic free Ca²⁺ with presence of HANB (1mM)

Chapter 4 Discussion

4.1 Chemical Synthesis

Both NPPB and the structural analogues were synthesized, the latter because they are not commercially available. NPPB was also bought commercially. The synthetic method presented in this research is based on a simple reductive amination of an aldehyde with a primary amine, which is a relatively simple procedure and does not require a high temperature. The reductive amination reaction enabled the synthesis of NPPB and a variety of structurally related compounds with the use of different aldehyde and amine starting materials.

In this research, NPPB, PPAB, HANB, and HANB-2 were synthesized. There have been previous reports of the synthesis of NPPB, PPAB and HANB, based on the reductive amination reaction (50,54). Although slight improvement of purification procedure was suggested, total yields of these compounds in this research were close or slightly better than the previous research, which supports the use of the reductive amination method to establish a library of NPPB and related compounds. Furthermore, the first synthesis of HANB-2 was performed and the purity of compound was confirmed by chemical data, such as ^1H NMR, ^{13}C NMR, mass spectra (MS) and infrared spectra (IR). This again suggests that the reductive amination method is suitable for the production of a range of related compounds.

4.1.1 NPPB

The product of NPPB synthesis was bright yellow and gave a 53.26% yield, while previous studies showed a 52% yield. Although the existing literature suggests the use of column chromatography to purify NPPB (50), almost all of

the impurities were removed by the one step of re-crystallization with methanol and water, rather than column chromatography. Therefore, re-crystallization is a more efficient methodology than column chromatography to purify the product of NPPB in high yield.

4.1.2 PPAB

PPAB is an NPPB analogue which has the 5-nitro group removed from the benzoate ring. The product was white and produced a 54.04% yield. A previous study gave a 52% yield (Giles *et al* 2003, personal communication). Almost all impurities were removed by the column chromatography. However, some impurities were still observed by the ¹H NMR. Therefore column chromatography is suitable to purify PPAB, but re-crystallization is still required to yield pure product.

4.1.3 HANB

HANB is an NPPB analogue which has the phenyl group missing from the end of the aliphatic chain. The aliphatic chain in HANB is slightly longer than NPPB as the heptaldehyde is used as starting material. The product is dark yellow colour and produced a 53.72% yield, while previous study showed a 49% yield (Giles *et al* 2003, personal communication). As for PPAB, HANB can also be purified efficiently by column chromatography, but it still requires re-crystallization to yield pure product.

4.1.4 HANB-2

HANB-2 is a NPPB analogue which is also has the phenyl group removed the same as HANB. The position of carboxyl-group is, however, shifted in this analogue relative to HANB. The product did not form crystals and it remained as a brown coloured oily type residue. Purification of this proved extremely

difficult. After several different types of chromatography, the product was purified to a 67.58% yield, which was assessed by ^1H NMR, ^{13}C NMR, mass spectra (MS) and infrared spectra (IR). This is the first synthesis of HANB-2. The yield of pure HANB-2 supports the effectiveness of the reductive amination method for synthesizing a large variety of NPPB analogues.

The significance of this analogue is the shifted position of carboxylate group. The carboxylate in this molecule acts as an anionic group, which is ionized at physiological pH. This carboxylate anion state has a crucial role for the acidity of the molecule, which may be necessary for the potency of the molecule as the ion channel inhibitor. This is supported by the fact that the absence of the benzoate ring (2-amino-4-phenylbutyric acid) resulted in a complete absence of inhibitory function toward CFTR Cl^- channel activity (5).

Unfortunately, HANB-2 was not able to be tested in any biological experiments in this research, because of its insolubility in water. HANB-2 was only soluble in 100% ethanol. Further investigation for the analysis of HANB-2 is required.

4.2 Cytoplasmic Streaming

Cytoplasmic streaming is the circular flow of cytoplasm, with the coordinated movement of particles, vacuoles, and other organelles through the cytosol. It is sensitive to changes in ion concentrations and fluxes across cell membranes. The effects of ion channel inhibitors on cytoplasmic streaming rates were studied. When a high concentration of NPPB, purchased from Sigma Chemicals, was applied to the internodal cells of *Nitella hookeri*, total cessation of cytoplasmic streaming occurred. This was followed by cell death.

The cessation of cytoplasmic streaming is thought to be induced by increased cytosolic Ca^{2+} levels, which may also be involved in part with the apoptotic cell death mechanism. The possible inhibition of K^+ and Cl^- channels caused by the presence of NPPB and related compounds may have induced a change of membrane potential, which activates an increase of cytosolic Ca^{2+} levels.

The effect of NPPB and related compounds on cytoplasmic streaming rate in the alga *Nitella hookeri* has been previously documented (54). The ability of NPPB and related compounds to slow down or cease cytoplasmic streaming was observed to ascertain in the effects of structural modification of NPPB. According to this research, cytoplasmic streaming in *Nitella hookeri* was sensitive to NPPB, PPAB and HANB with IC_{50} values of $24\mu\text{mol/L}$, $455\mu\text{mol/L}$, and 6.4mmol/L , respectively.

These results suggested the importance of the nitro and phenyl groups in the structure of NPPB molecule. Removal of nitro group, forming PPAB, gave higher IC_{50} value than NPPB, which means that PPAB is less potent than NPPB. The importance of nitro group on potency of NPPB was also supported by Walsh *et al* who found that removal of nitro group decreased the potency of NPPB toward blockage of the CFTR Cl^- channel. On the other hand, removal of phenyl group appears even more crucial, because HANB showed a greater increased IC_{50} value. This does not agree with CFTR study by Walsh *et al*, which suggested that the nitro group is more important than the phenyl group. During turgor regulation and cytosolic Ca^{2+} analysis in this research, however, the solubility of HANB was always a concern. The insolubility of HANB in water may interrupt the activity of inhibition, consequently it may show a much higher IC_{50} value. Although some results suggested differences in the

relative importance of the functional groups, the findings have identified that both groups are required for optimal activity of NPPB.

To support the significance of cytoplasmic streaming study for a single preliminary assay for studying the effects of structural modifications of NPPB, NPPB and niflumic acid purchased from Sigma Chemicals were tested on cytoplasmic streaming in *Nitella hookeri*, while the existing literature used synthesized NPPB. The cytoplasmic streaming rate after 5 minutes and 10 minutes immersion in pH 8 and 10 NPPB solutions showed no significant difference according to the t-test result which gave $P > 0.05$. Therefore, the IC_{50} value of purchased NPPB was stated as $88.65 \mu\text{mol/L}$, while IC_{50} value of niflumic acid was $121.82 \mu\text{mol/L}$. Although the IC_{50} value of purchased NPPB showed a slight different from that of synthesized NPPB, the results showed that the effect of ion channel inhibitors, such as NPPB and niflumic acid, on cytoplasmic streaming, provides a simple assay system for analyzing the effects of structural modification ion channel inhibitors.

4.3 Turgor Regulation

4.3.1 Turgor Pressure in Resting State

The steady-state turgor pressure of internodal cells of *Nitella hookeri* measured using a single cell pressure probe was 7.44MPa . This value is in close agreement with that reported in a previous study of the closely related species *Nitella flexilis*, which was reported to have a turgor pressure around $7\text{--}8 \text{MPa}$ in the steady-state (55). This suggests that the pressure probe measurements performed in this report was adequate technique for turgor regulation study of internodal cells.

4.3.2 Hypertonic Regulation

The turgor regulation under high osmotic stress, established by immersion of internodal cells to APW containing 100mM of sorbitol, was observed. Osmotic stress is a constant challenge for higher plants including freshwater algae. One of the immediate effects of osmotic stress is the change in the electrical properties of the plasma membrane followed by turgor regulation caused by large changes in the net ion fluxes across the plasma membrane. This transport of solutes establishes an osmotic gradient that causes a corresponding flow of water and change in the turgor pressure. Therefore, the turgor pressure tends to be reduced with hyperosmotic shock. In this report, the internodal cells of *Nitella hookeri* exposed to hyperosmotic stress reduced the turgor pressure from 7.44MPa to 5.08-4.82MPa, this being caused by movement of water out of the cell from a low to a high concentration of solutes. At higher sorbitol concentrations (higher than 100mM) the cells lost rigidity and were not able to be impaled by the microcapillaries. Presumably, the cells immersed in such high concentrations of sorbitol solution will show greater reductions of turgor pressure.

In plant cells, it is most likely that the turgor pressure is controlled. Thus an initial reduction in turgor pressure should then show an increase as cells restore to the value to the initial level or the steady-state by controlling net ion fluxes by activated membrane transport proteins, such as ion channels and pumps. A model of a potential turgor regulation mechanism based on studies of *Arabidopsis* root cells (69) is illustrated in Fig 4.1.

The turgor pressure of sample cells under hyperosmotic stress, which was 5.08-4.82MPa, and was measured 30 minutes after the cells were immersed in the hyperosmotic solution. Although there was 30 minutes from the initial

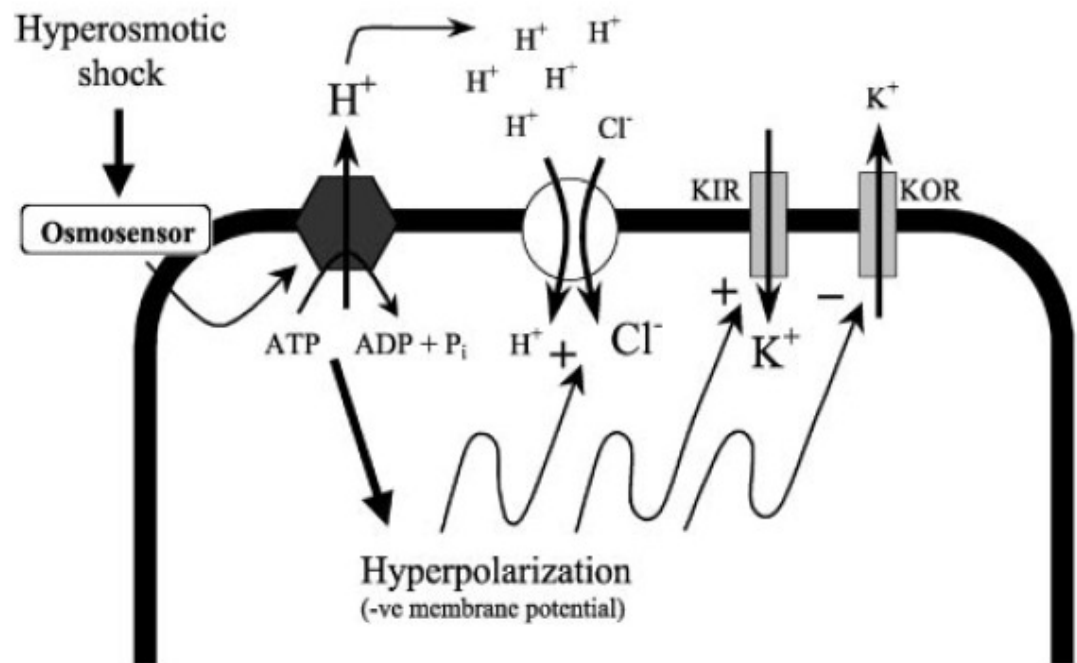


Figure 4.1 A model illustrating pathways of fast turgor adjustment in Arabidopsis root cells. Hyperosmotic shock, sensed via an osmosensor, activates the H⁺-ATPase. The hyperpolarisation increases net K⁺ uptake through an inward K⁺ channel and concomitantly decreases K⁺ efflux through an outward K⁺ channel. Both the hyperpolarized potential and extracellular acidification increase uptake of Cl⁻ through a H⁺/Cl⁻ symporter. (Adapted from (69))

osmotic shock, the measurement still showed a reduction of turgor pressure. It has been reported that the recovery of turgor pressure from osmotic shock tends to take time. In a study of *Arabidopsis* root hairs, the turgor pressure dropped in response to hyperosmotic stress, and turgor recovery took a period of about 30 minutes (56). Another study of *Ventricaria ventricosa*, the reduced turgor pressure recovered to the steady state in 314 minutes (70). Also, some cells started regulation immediately, others took up to 90 minutes to begin.

In the current research, the turgor pressure measurement of the internodal cells under hyperosmotic stress did not attempt to identify the time required for turgor regulation. The results, which represent measurements taken 30 minutes after the initial osmotic shock, were not identified as initial reduction of turgor pressure or partially recovered. However, it has been exploited as control experiments for observing the effects of ion channel inhibitors on the turgor regulation.

4.3.3 Effects of Ion channel inhibitors

The effects of application of the ion channel inhibitors, NPPB and PPAB, on turgor reduction of plant cells in hyperosmotic solution were studied. Both inhibitors showed effects on turgor regulation as shown by inhibition of the turgor pressure reduction caused by hyperosmotic shock. In other words, the presence of ion channel inhibitors may enhance recovery of turgor pressure. Alternatively they may simply reduce the initial reduction of turgor itself.

Shabara *et al* reported the enhancement of turgor regulation of *Arabidopsis* root hair cells, which showed completely recovery of turgor pressure in 40-50 minutes from hyperosmotic shock, while mung bean root cells took 6 hours to complete (71). The study of *Arabidopsis* root cells suggested that osmotically

induced uptake of inorganic ions is an important (and apparently predominant) component of fast turgor recovery. It has been reported that osmotic adjustment is an energy consuming process. The osmotic stress causes rapid, significant, and prolonged hyperpolarisation of plasma membrane potential. The activity of the electrogenic ATP-dependent H^+ pump is the major source for generating the membrane potential in higher plant cells. It is not surprising that such a pump has important role for osmotic adjustment. This is supported by experiments with specific inhibitors of ATPase activity.

The hyperpolarisation caused by osmotic stress, activates voltage-gated K^+ channels and increase K^+ influx. As an alternative, outward K^+ channels may be partially shut down, reducing K^+ efflux, which is consistent with the decreased conductance after hyperosmotic treatment reported by (72). Another report also suggested that the reduction of K^+ efflux took place rather than stimulation of K^+ influx in cultured Arabidopsis cells during osmotic stress adjustment (73).

Although the experiments in this research do not provide great details of inhibition mechanism, the presence of NPPB or PPAB as ion channel inhibitor for K^+ may reduce K^+ efflux during turgor regulation. Consequently, the cells immersed in the hyperosmotic solution with NPPB or PPAB showed faster recovery of turgor pressure than the one without inhibitors. The results were only preliminary to state that NPPB and PPAB inhibit only outward K^+ channels. Even though NPPB and PPAB inhibit both inward and outward K^+ channels, there may be other effectors that also induce ion uptake. The K^+ influx is strongly enhanced by ATP-dependent H^+ pump activity. Furthermore, a K^+ pump, which is activated by low turgor pressure, has been identified on tonoplasts (70). Therefore, the effects of NPPB and PPAB on the turgor

regulation are able to be explained as reduction of K^+ efflux during osmotic stress, which leads to faster recovery of turgor regulation.

Both NPPB and PPAB showed the activity in dose dependent manner. However, PPAB showed less potency than NPPB. This result agrees with IC_{50} value during the cytoplasmic streaming experiments, which showed lower IC_{50} values for NPPB than for PPAB.

4.4 Cytosolic Free Calcium Analysis

The effects of NPPB and related compounds on cytosolic free Ca^{2+} levels of *Nicotiana plumbaginifolia* plants were determined using aequorin technology. Calcium influx was induced by cold shock treatment. The average of increased cytosolic Ca^{2+} level induced by cold shock was used as a control. The presence of NPPB and PPAB reduced the cold shock induced cytosolic Ca^{2+} level in a dose dependent manner, while HANB showed no effect. However, the relevance of the use of aequorin technology for testing HANB is questionable. The quantitative analysis of Ca^{2+} in the cytosol using aequorin technology is reliant on the luminescence measurements of the emitted light from the aequorin complex upon binding of Ca^{2+} . Because HANB has a tendency to absorb the blue light, which is released from the aequorin complex, the ability to absorb the light would thus affect the accuracy of the results. Therefore, the ineffectiveness of HANB on the plasma membrane Ca^{2+} channel may be caused by the light absorbing ability of the HANB molecules and not by any lack of any inhibitory effect of HANB itself.

NPPB and PPAB reduced the cold shock induced cytosolic Ca^{2+} level in a dose dependent manner with an estimated effective dose somewhere between

75 to 100 μ M for NPPB and 100 μ M to 1mM for PPAB. Such results may be indicative of NPPB and PPAB having an inhibitory effect on Ca²⁺ ion channel activities. However, NPPB and PPAB are well known as Cl⁻ and K⁺ ion channel inhibitors and their mode of action as these is well documented. The blockage of Cl⁻ and K⁺ ion channels could affect membrane potential which in turn is likely to be an elicitor of Ca²⁺ flux. It is currently not possible to conclude whether the effects of the inhibitors on Ca²⁺ flux are direct (i.e. via Ca²⁺ channels) or indirect (i.e. via changes in membrane potential). Clearly this is an area where direct patch clamp experiments are required.

However, it is also pertinent to consider the results of the cytoplasmic streaming analysis. The presence of NPPB and PPAB slowed down the cytoplasmic streaming rate of *Nitella hookeri*. A cessation or slow down of cytoplasmic streaming caused by an increase of the cytoplasmic Ca²⁺ level has previously been reported (53). Therefore the presence of NPPB and PPAB would be predicted to induce Ca²⁺ influx, whereas the contrasting result of a reduction of cytosolic Ca²⁺ level with presence of NPPB and PPAB was observed by direct measurement of cytosolic free Ca²⁺ level of *Nicotiana plumbaginifolia* using aequorin technology.

In comparing the results of the cytoplasmic streaming analysis and cytosolic Ca²⁺ analysis, it should be noted that the stimuli of Ca²⁺ fluxes were different during each experiment. In the cytoplasmic streaming analysis, NPPB and PPAB themselves were stimuli for the Ca²⁺ fluxes that led to the reduction of streaming rate. On the other hand, in the cytosolic Ca²⁺ analysis, cold shock treatment was a stimulus for increasing cytosolic Ca²⁺ levels. The mechanism of elevation of cytosolic free Ca²⁺ level might be different, since there are a number of potential Ca²⁺ sources, such as the extracellular medium, vacuoles,

other organelles and the cell wall. Also a variety of different kinds of ion channels, such as voltage-insensitive channels may be responsible for Ca^{2+} movements. Consequently the action of NPPB and PPAB toward the Ca^{2+} fluxes might be different in the two experiments.

The results from the cytosolic free Ca^{2+} analysis in this report are still preliminary, and further research will be required to testify the mode of action of NPPB and related compounds. However, the measurement of the cytosolic free Ca^{2+} level can be used as a more direct measure of the inhibitory effect, while the cytoplasmic streaming analysis is a more indirect method. As detailed above there is clearly a need for further study perhaps involving direct patch clamp measurement of the inhibitory effect of the compounds on channels of known identification. Such studies are however difficult and usually are suitable for higher level research than MSc.

Chapter 5 Conclusions and Future Research

NPPB and related compounds, such as PPAB, HANB and HANB-2, were synthesised by using reductive amination procedures, with modifications these were able to give slightly higher yields than those previously reported. The reductive amination procedures were readily simple and easy to perform and can be used to establish a chemical library of the compounds such as NPPB.

A cytoplasmic streaming assay, using giant green algae, has already been suggested as a suitable preliminary assay for studying the effects of structural modifications of ion channel inhibitors, such as NPPB. This has been confirmed in the present study by using commercial NPPB and niflumic acid, which also showed the effect on cytoplasmic streaming rate of slowing down or cessation of the streaming. These effects occurred in a dose dependent manner.

Turgor regulation study with hyperosmotic shock was also suggested as a simple assay for studying the inhibitory effects of ion channel inhibitors. The presence of NPPB and PPAB seem to enhance turgor regulation, enabling a fast recovery from the hyperosmotic shock.

Cytosolic free Ca^{2+} analysis, using aequorin technology, can be used as a more direct measurement of any inhibitory effect on Ca^{2+} channels, while the cytoplasmic streaming analysis and turgor regulation analysis are more indirect methods. The presence of NPPB and PPAB reduced the cold shock induced cytosolic Ca^{2+} increases in a dose dependent manner.

The results from this report are still preliminary, and further research will be required to elucidate in more detail the mode of action of NPPB and related compounds, this would perhaps involve direct patch clamp measurement of the inhibitory effect of the compounds on channels of known identification. However, this research clearly supports the suggestion that a study of the effects of structural modifications of ion channel inhibitors on cytoplasmic streaming, turgor regulation, and cytosolic Ca^{2+} analysis can be used as simple preliminary assays, which can provide the indication for further research.

References

1. Taiz, L., and Zeiger, E. (1991) *Plant physiology*, 1 Ed., Sinauer Associates, Inc, Sunderland, Massachusetts
2. Coleman, H. A. (1986) *Journal of Membrane Biology* 93(1), 55-61
3. Garrett, R. H., and Grisham, C. M. (1999) *Biochemistry*, 2 Ed., Saunders College Publishing
4. Van Winkle, L. J. (1995) *Biomembrane Transport*, Academic Press, New York
5. Ma, T., Thiagarajah, J. R., Yang, H., Sonawane, N. D., Folli, C., Galletta, L. J. V., and Verkman, A. S. (2002) *J. Clin. Invest.* 110(11), 1651-1658
6. Campbell, N. A., Reece, J. B., and Mitchell, L. G. (1999) *Biology*, 5 Ed., Addison Wesley Longman Inc
7. Hille, B. (2001) *Ion Channels of Excitable Membranes*, 3 Ed., Sinauer Associates Inc
8. Molleman, A. (2003) *Patch Clamping*, John Wiley & Sons LTD
9. Sibaoka, T. T. (1966) *Symposium of the Society of Experimental Biology* 20, 49-73
10. Samejima, M., and Sibaoka, T. (1982) *Plant Cell Physiol.* 23(3), 459-465
11. Kikuyama, M. (2001) Role of Ca²⁺ in membrane excitation and cell motility in characean cells as a model system. In. *International Review of Cytology*, Academic Press
12. Tester, M. (1990) *New Phytologist* 114(3), 305-340
13. Sokolik, A. I., and Yurin, V. M. (1986) *Journal of Membrane Biology* 89(1), 9-22
14. Tester, M. (1988) *Journal of Membrane Biology* 103(2), 159-169

15. Bertl, A. (1989) *Journal of Membrane Biology* 109(1), 9-19
16. Laver, D. R. (1990) *Journal of Membrane Biology* 118(1), 55-67
17. Laver, D., and Walker, N. (1987) *Journal of Membrane Biology* 100(1), 31-42
18. Laver, D. R., and Walker, N. A. (1991) *Journal of Membrane Biology* 120(2), 131-139
19. Luhning, H. (1999) *Journal of Membrane Biology* 168(1), 47-61
20. Lunevsky, V. Z., Zherelova, O. M., Vostrikov, I. Y., and Berestovsky, G. N. (1983) *Journal of Membrane Biology* 72(1 - 2), 43-58
21. Shimmen, T., and Nishikawa, S.-i. (1988) *Journal of Membrane Biology* 101(1), 133-140
22. Tyerman, S. D., Findlay, G. P., and Paterson, G. J. (1986) *Journal of Membrane Biology* 89(2), 139-152
23. Tyerman, S. D., Findlay, G. P., and Paterson, G. J. (1986) *Journal of Membrane Biology* 89(2), 153-161
24. Falke, L. C., Edwards, K. L., Pickard, B. G., and Mislser, S. (1988) *FEBS Letters* 237(1-2), 141-144
25. Bush, D. S. (1995) *Annual Review of Plant Physiology and Plant Molecular Biology* 46(1), 95-122
26. White, P. J., and Broadley, M. R. (2003) *Ann Bot* 92(4), 487-511
27. White, P. J. (2000) *Biochimica et Biophysica Acta (BBA) - Biomembranes* 1465(1-2), 171-189
28. Thuleau, P., Moreau, M., Schroeder, J. I., and Ranjeva, R. (1994) *The EMBO Journal* 13(24), 5843-5847
29. Thion, L., Mazars, C., Nacry, P., Bouchez, D., Moreau, M., Ranjeva, R., and Thuleau, P. (1998) *The Plant Journal: For Cell And Molecular Biology* 13(5), 603-610
30. White, P. J. (1998) *Ann Bot* 81(2), 173-183

31. Taylor, L. P., and Hepler, P. K. (1997) *Annual Review of Plant Physiology and Plant Molecular Biology* 48(1), 461-491
32. Zimmermann, S., Nurnberger, T., Frachisse, J.-M., Wirtz, W., Guern, J., Hedrich, R., and Scheel, D. (1997) *PNAS* 94(6), 2751-2755
33. Evans, D., Hallwood, K.S, Cashin, C.H, Jackson, H. (1967) *Journal of Medicinal Chemistry* 10(3), 428-431
34. Landry, D. W., Reitman, M, Cragoe, E. J. Al-Awqati, Q. (1987) *The Journal of general physiology* 90, 779-798
35. Marten, I., Zeilinger C, Redhead C, Landry DW, al-Awqati Q, Hedrich R. (1992) *The EMBO Journal* 11(10), 3569-3575.
36. Sauer, G., Simonis, W., and Schmitt-Knecht, G. (1993) *Plant Cell Physiol.* 34(8), 1275-1282
37. Thiel, G. H., U. Plieth, C. . (1997) *JOURNAL OF EXPERIMENTAL BOTANY* 48(308/SPI), 609-622
38. Myssina, S., Lang, P. A., Kempe, D. S., Kaiser, S., Huber, S. M., Wieder, T., and Lang, F. (2004) *Cellular Physiology and Biochemistry* 14(4-6), 241-248
39. Fioretti, B., Castigli, E., Calzuola, I., Harper, A. A., Franciolini, F., and Catacuzzeno, L. (2004) *European Journal of Pharmacology* 497(1), 1-6
40. Ottolia, M., and Toro, L. (1994) *Biophys. J.* 67(6), 2272-2279
41. Gogelein, H., Dahlem, D., Englert, H. C., and Lang, H. J. (1990) *FEBS Letters* 268(1), 79-82
42. Stuart, F. C., Lynne, M. B., and Robert, M. D. (2003) *British Journal of Pharmacology* 140(8), 1442
43. Garrill, A., Tyerman, S.D, Findlay, G.P and Ryan, P.R. . (1996) *Australian Journal of Plant Physiology* 23(4), 527-534

44. Greger, R., and Sidney Fleischer and Becca, F. (1990) [45] Chloride channel blockers. In. *Methods in Enzymology*, Academic Press
45. Walsh, K. B., and Wang, C. (1996) *Cardiovascular Research* 32(2), 391-399
46. Walsh, K. B., Long, K. J., and Shen, X. (1999) 127(2), 369-376
47. Choi, K. L., Mossman, C., Aube, J., and Yellen, G. (1993) *Neuron* 10(3), 533-541
48. Wangemann, P., Wittner, M., Di Stefano, A., Englert, H. C., Lang, H. J., Schlatter, E., and Greger, R. (1986) *Pfluegers Arch* 407(Suppl 2), S128-S141
49. Branchini, B. R., Murtiashaw, M. H., and Egan, L. A. (1991) *Biochemical and Biophysical Research Communications* 176(1), 459-465
50. Giles, K. R., Humphries, M., Abell, A., and Garrill, A. (2003) *Bioorganic & Medicinal Chemistry Letters* 13(2), 293-295
51. Borch, R. F., Bernstein, M. D., and Durst, H. D. (1971) *Journal of the American Chemistry Society* 93, 2897-2904
52. Mattson, R. J., Pham, K. M., Leuck, D. J., and Cowen, K. A. (1990) *Journal of Organic Chemistry* 55, 2552-2554
53. Kikuyama, M., Shimada, K., and Hiramoto, Y. (1993) *Protoplasma* 174(3 - 4), 142-146
54. Graichen, F., Giles, K. R., Abell, A., and Garrill, A. (2005) *Biochemistry and Cell Biology* 83(2), 133
55. Findlay, G. P. (2001) *Australian Journal of Plant Physiology* 28(7), 619-636
56. Lew, R. R. (2004) *Plant Physiol.* 134(1), 352-360
57. Lew, R. R., Levina, N. N., Walker, S. K., and Garrill, A. (2004) *Fungal Genetics and Biology* 41(11), 1007-1015

58. Messiaen, J., Read, N. D. V., Cutsem, P., and Trewavas, A. J. (1993) *J Cell Sci* 104(2), 365-371
59. Knight, M. R., Campbell, A. K., and et al. (1991) *Nature* 352(6335), 524
60. Lecourieux, D., Ranjeva, R., and Pugin, A. (2006) *New Phytologist* 171(2), 249-269
61. Armarego, W. L. F., and Chai, C. L. L. *Purification of Laboratory Chemicals*, 5 Ed.
62. Chandra, S., and Low, P. S. (1997) *J. Biol. Chem.* 272(45), 28274-28280
63. Lecourieux, D., Mazars, C., Pauly, N., Ranjeva, R., and Pugin, A. (2002) *Plant Cell* 14(10), 2627-2641
64. Chandler, M., Tandeau de Marsac, N., and Kouchkovsky, Y. (1972) *Canadian Journal of Botany-Revue Canadienne de Botanique* 50, 2265-2270
65. Binet, M.-N., Humbert, C., Lecourieux, D., Vantard, M., and Pugin, A. (2001) *Plant Physiol.* 125(2), 564-572
66. Allen, D. G., Blinks, J. R., Prendergast, F. G. . (1976) *Science* 195, 996-998
67. van der Luit, A. H., Olivari, C., Haley, A., Knight, M. R., and Trewavas, A. J. (1999) *Plant Physiol.* 121(3), 705-714
68. Williams, D. H., and Fleming, I. (1973) *Spectroscopic methods in Organic Chemistry*, 2 Ed., McGraw-Hill Book Company (UK) Limited
69. Shabala, S. N., and Lew, R. R. (2002) *Plant Physiol.* 129(1), 290-299
70. Bisson, M. A., and Beilby, M. J. (2004) *Journal of Membrane Biology* 190(1), 43-56

71. Itoh, K., Nakamura, Y., Kawata, H., Yamada, T., Ohta, E., and Sakata, M. (1987) *Plant Cell Physiol.* 28(6), 987-994
72. Lew, R. R. (1996) *Plant Physiol.* 112(3), 1089-1100
73. Zingarelli, L., Teresa Marre, M., Massardi, F., and Lado, P. (1999) *Physiologia Plantarum* 106(3), 287-295